THESIS APPROVAL

GRADUATE SCHOOL, KASETSART UNIVERSITY

Doctor of Philosophy (Genetic Engineering)
DEGREE

Genetic Engineering — **FIELD**

Interdisciplinary Graduate Program — **PROGRAM**

TITLE: Genomic Analysis and Molecular Breeding for High Grain Iron Density and Iron Bioavailability in Rice

NAME: Mr. Siriphat Ruengphayak

THIS THESIS HAS BEEN ACCEPTED BY

(Associate Professor Apichart Vanavichit, Ph.D.) **THESIS ADVISOR**

(Mr. Somvong Tragoonrung, Ph.D.) **COMMITTEE MEMBER**

(Associate Professor Ratchanee Kongkachuichai, Ph.D.) **COMMITTEE MEMBER**

(Assistant Professor Siriwan Prapong, Ph.D.) **GRADUATE COMMITTEE CHAIRMAN**

APPROVED BY THE GRADUATE SCHOOL ON _____

(Associate Professor Gunjana Theeragool, D.Agr.) **DEAN**

THESIS

GENOMIC ANALYSIS AND MOLECULAR BREEDING FOR HIGH GRAIN IRON DENSITY AND IRON BIOAVAILABILITY IN RICE

SIRIPHAT RUENGPHAYAK

A Thesis Submitted in Partial Fulfillment of
the Requirements for the Degree of
Doctor of Philosophy (Genetic Engineering)
Graduate School, Kasetsart University
2014

Siriphat Ruengphayak 2014: Genomic Analysis and Molecular Breeding for High Grain Iron Density and Iron Bioavailability in Rice. Doctor of Philosophy (Genetic Engineering), Major Field: Genetic Engineering, Interdisciplinary Graduate Program. Thesis Advisor: Associate Professor Apichart Vanavichit, Ph.D. 87 pages.

Rice contains the lowest grain Fe content among cereals. One biological limiting factor is the tolerance of rice to Fe toxicity. Two sources of genetic variation, natural and mutants, were utilized in this study. No significant improvement in grain Fe content by phenotypic selection using natural genetic variants as donor. Mutagenized population was developed by fast neutron irradiation and was fixed in four self-pollination. Reverse and forward genetics screenings were designed for identification of high grain Fe density and tolerance to Fe toxicity in M_2 to M_4 populations.

Two types of mutants related to Fe content and Fe toxicity were successfully isolated by forward screening of 12,000 mutagenized lines. Among PPB screened lines so far, 76 mutants contained higher grain Fe density, while only 2 mutants were very low. The Fe grain density was varied from 29 ppm (Mu4643) to 7 ppm (Mu8097). On the other hand, screening for Fe toxicity tolerance at 300 ppm Fe toxic level identified 95 tolerance and 57 susceptible lines compared to the wild type. Moreover, coding sequence amplicons were genotyped on six iron homeostatic genes by using denaturing high performance liquid chromatography (dHPLC). Five mutants were identified in *OsFRO1* (LOC_Os04g36720). One such mutant called 'MuFRO' accumulated 21-30 % more grain Fe content than its wild type on both normal and toxic levels of Fe. To search for mutated genes at the whole genome level, Single Feature Polymorphism (SFP) followed by sequencing revealed four candidate genes for cation transporters, *OsPDR3*, Zinc finger, *OsI-3-GPL* and *OsLLS1*, were distinctively different between the low and high grain Fe content mutants wild type.

_____ / ___ / ___

Student's signature Thesis Advisor's signature

ACKNOWLEDGEMENTS

I would like to gratefully thank and deeply indebted to Assoc. Prof. Dr. Apichart Vanavichit my thesis advisor for advice, encouragement and valuable suggestion for completely writing of thesis. I would sincerely like to thank Dr. Somvong Tragoonrung, and Assoc. Prof. Dr. Ratchanee Kongkachuichai my committees, and also Dr. Tida Amon external examiner for their valuable comments and suggestion. I gratefully thank Dr. Theerayut Toojinda for valuable suggestions. I gratefully thank to Dr. Vinitchan Ruanjaichon for kind advices. I gratefully thank all member staffs of Rice Science Center and Rice Gene Discovery Unit, Kasetsart University, Kamphaeng Saen, Nakhon Pathom.

This research was supported The Royal Golden Jubilee (RGJ)-PhD program Grant No. PHD / 0009 / 2546, from the Thailand Research Fund (TRF), the National Research Council of Thailand (NRCT) and the National Center for Genetic Engineering and Biotechnology (BIOTEC)

Finally, my deepest gratitude goes to my beloved parent and my family. All of their unfailing love, sacrifices and abundant support made this long journey of my study in a doctor of philosophy (Genetic Engineering) at Kasetsart University successful completed.

Siriphat Ruengphayak

October 2013

TABLE OF CONTENTS

Page

LIST OF TABLES

LIST OF TABLES (Continued)

LIST OF FIGURES

LIST OF FIGURES (Continued)

LIST OF FIGURES (Continued)

Appendix Figure

LIST OF FIGURES (Continued)

LIST OF ABBREVIATIONS

AAS	=	Atomic Absorption
bp	=	base pair
CTAB	=	Cetyl trimethyl ammonium bromide
DAF	=	Day after fertilization
DHPLC	=	Denaturing High Performance Liquid Chromatography
DNA	=	Deoxyribonucleic acid
EMS	=	Ethyl methanesulfonate
Fe^{2+}	=	Ferrous ion
Fe^{3+}	=	Ferric ion
FN	=	Fast neutrons
ICP	=	Inductively coupled plasma
IDA	=	Iron deficiency anemia
In/Del	=	Insertion/Deletion
JHN	=	Joa Hom Nin
mg/l	=	Milligram per liter
ml	=	Mililiter
MuFRO	=	*Ferric chelate reductase* mutant
ng/µl	=	Nanogram/ µl
OsCaO	=	*chlorophyll a oxygenase (CaO)*
OsFRO1	=	*Ferric-chelate reductases1*
OsFer1	=	*Ferritin1*
OsFer2	=	*Ferritin2*
OsI-3-GPL	=	*Indole-3-glycerol phosphate lyase*
OsIRT1	=	*Iron regulate transpoter1*
OsLLS1	=	*lethal leaf spot1*
OsNAS3	=	*Nicotinamide synthase3*
OsPDR3	=	*Pleiotropic drug resistance protein*
OsYSL1	=	*Yellow-stripe like1*
PCR	=	Polymerase Chain Reaction

LIST OF ABBREVIATIONS (Continued)

PPB	=	Perl Prussian Blue
ppm	=	Part per million
RNA	=	Ribonucleic acid
RT-PCR	=	Reverse Transcriptase Polymerase Chain Reaction
SFP	=	Single feature polymorphism
SNP	=	Single nucleotide polymorphism
SAP	=	Single amino acid polymorphism
TILLING	=	Targeting induced local lesions in genomes
µl	=	Microliter
µM	=	Micromole
ºC	=	Degree Celsius

GENOMIC ANALYSIS AND MOLECULAR BREEDING FOR HIGH GRAIN IRON DENSITY AND IRON BIOAVAILABILITY IN RICE

INTRODUCTION

Iron (Fe)-deficiency anemia is one of the most prevalent human micronutrient deficiencies in the world, affecting an estimated one-third of the world's population (WHO, 2002). To address this problem, improvement of high grain Fe density and bioavailability is advantageous for people who experience difficulty in changing their diet.

In the rice consuming world, as people normally taking 200-400 g of polished rice daily, nutritious rice grains can become a main ingredient in designer foods that tailor-made for the future world. Thus, understanding the mechanisms of Fe uptake and translocation in rice is of utmost importance in the development of rice varieties with high grain iron.

Rice and others graminaceous monocots were secreted small molecules called mugineic acid family phytosiderophores (MAs) that solubilize Fe on the root surface (Takagi 1976). These compounds act as chelators of ferric ions and are taken up by root cells as Fe (III)-phytosiderophore complexes (Curie *et al.,* 2001; Nozoye *et al.,* 2011). The mechanisms underlying Fe transport and homeostasis have been involved, providing opportunities to increase the Fe content in rice grain. As excess Fe is toxic to cells, plants have developed complex mechanisms to absorb Fe from soil and to transport it from root to shoot and grain. At the present time, many reports have been made in elucidating the MA biosynthetic pathway, identifying proteins that transport Fe in various forms, and exposing the transcription factors controlling the Fe homeostasis (Nishizawa *et al.*, 2010).

A lack of iron in plants diet is often causing of IDA, especially in the vegetarians and many poorer families. Because non-heme iron is also found in rice and plants had lower bioavailability than heme iron from animal tissue (Lucca *et al.,* 2001). The bioavailability of non-heme iron is greatly influenced by both dietary inhibitors and enhancers (Hallberg *et al.,* 1989 and Yang *et al.,* 2006**)**. The balance between absorption facilitators and inhibitors, along with the existing iron status of the individual determines the bioavailability of iron from individual foods or from a meal. Amino acids (especially cysteine), ascorbic acid, citric acid, and fructose can enhance iron absorption, while some organic compounds include phytate, polyphenols, oxalate, tannin, and calcium can inhibit the iron absorption (Tuntawiroon *et al.,* 1991).

Iron biofortification in rice without GMOs can be done either through natural genetic variation selection and mutagenesis. Improvement of nutritional quality traits, sometime there are not enough a natural variation. Mutation breeding based-on TILLING, a non-transgenic method for reverse genetic, is an effective tool for nutritional enrichment rice breeding.

As a whole, this study on the generating new and useful sources of genetic variation based on mutagenesis. The scopes of this research were involved grain iron density and its bioavailability candidate genes identification. And also identify permanent mutants conferring high grain Fe density and tolerance to Fe toxicity from Jao Hom Nin (JHN) mutant population. An artificial mutation is the utilize material for high grain rice breeding program.

OBJECTIVES

The aim of this study is to understand the mechanism and function of candidate genes controlling iron density and bioavailability in rice for developing rice strains with high grain iron.

The specific objectives are:

1. To collect iron mutant rice from JHN mutant population treated with fast neutron irradiation.

2. To locate genes/QTL for grain iron density and iron bioavailability on rice genome and identify sequence variation of candidate genes for effective marker development.

LITERATURE REVIEW

1. Grain iron density

Iron is the most abundant metal in the earth's crust, but iron is mainly found as stable Fe (III) compounds with low solubility at neutral pH (Guerinot and Yi, 1994; Welch, 1995; Lee and Sedlak, 2009), so plants are often deficient iron or chlorosis. Iron density of plant tissue is depending on iron acquisition (iron uptake and transport) and iron storage by plant. Breeding to enhance efficiency in these strategies can increase an iron density, especially in grain. However, excess iron is toxic, leading to oxidative stress and affected yield component. Therefore, plants must use finely tuned mechanisms to keep iron homeostasis in each of their organs, tissues, cells and organelles (Gross *et al*, 2003).

1.1 Iron acquisition and iron transport

Plants can be classified in two groups based on Iron (Fe) acquiring strategy (Marschner and Römheld, 1994). The strategy I, including dicotyledoneous and non graminaceous monocotyledoneous species take up iron similarly to yeast (Eide, 1998) by rhizosphere acidification, reduction of Fe^{3+} by ferric-chelate reductases such as *FRO2* (Robinson *et al.,* 1999) and import of Fe^{2+} across the plasma membrane in roots. In contrast, graminaceous monocots (strategy II plants) take up the iron by extruding low molecular mass secondary amino acids (phytosiderophores) that chelate sparingly soluble iron (Fe^{3+}) and uptake the Fe^{3+}-phytosiderophore complex by root (Briat and Lobreaux, 1997; Mori, 1999). The maize gene *yellow stripe1 (Ys1),* coding for a membrane protein with Fe^{3+}-phytosiderophore uptake activity, was cloned recently (Curie *et al.,* 2001).

Since iron acquisition, the nonproteinogenous amino acid nicotinamide (NA) found in all multicellular plants were considered to be a key component for both strategies for iron acquisition (Rudolph *et al.*, 1985). In strategy I plant, NA might

function as a chelator of iron in symplastic and phloem transport (Schmidke and Stephan, 1995). A similar role of NA is assumed for strategy II plants. Recently it was demonstrated that NA chelates both Fe (II) and Fe (III); these complexes are poor Fenton reagents, suggesting a role of NA in protecting cells from oxidative damage (Von Wirén *et al.*, 1999). In addition, in strategy II plants NA was shown to be a precursor for the biosynthesis of phytosiderophores of the mugineic acid family (Shojima *et al.*, 1985). In contrast to strategy II plants, the NA synthase (NAS) activity is not enhanced under iron deficiency in strategy I plants (Higuchi *et al.*, 1995; Herbik *et al.*, 1996; Herbik, 1997) suggesting that NAS activity is differently regulated in strategy I and II plants. However, NAS is a highly important enzyme for the regulation of the iron metabolism in both strategies I and II plants.

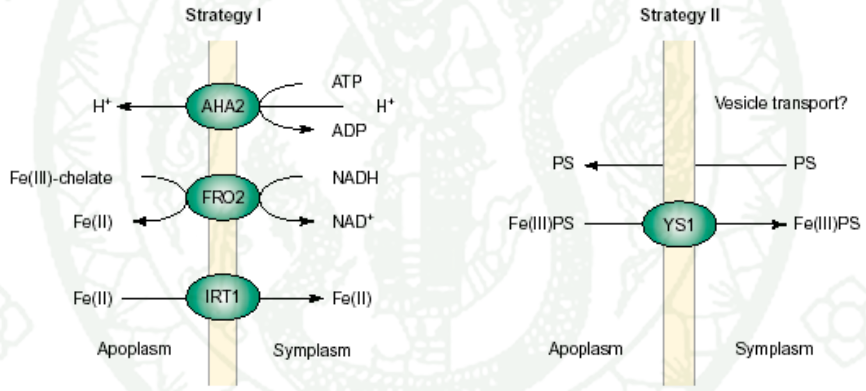

Figure 1 Mechanisms of iron acquisition in higher plants. In strategy I plants, Fe (III) chelates are reduced before the Fe (II) ion is transported across the plasma membrane. Strategy II plants release siderophores capable of solubilizing external Fe (III) and then transport the Fe (III) siderophore complex into the cell

Source: Rudiger and Stephan (2003)

It is generally believed that plants depend on a single system (either Strategy I or II) for iron acquisition. In graminaceous plants, such as barley and maize, the inducible Fe-deficiency Fe (II) transport system is either absent or is expressed only at very low levels (Zaharieva and Römheld, 2001). However, it's

possible that some plants have both uptake systems. For example, rice is a strategy II plant and releases phytosiderophores under Fe-deficiency, but under submerged conditions in paddy field where rice is normally grown, ferrous iron is more abundant than ferric iron, and rice can possess an iron uptake system for Fe (II) (Takagi, 1976). Isolation of a cDNA and genomic clone of *OsIRT1* studied the existence of a Fe (II) transport system for iron uptake in rice. *OsIRT1* has features typical of the ZIP metal transporter family, such as eight transmembrane domains and a variable region with a histidine-rich metal binding domain (Guerinot, 2000). Several members of this family have been isolated from dicotyledonous species (Eckhardt *et al*., 2001; Eide *et al*., 1996; Vert *et al.*, 2001). *OsIRT1* is the first member of the ZIP metal transporter family to be isolated from a graminaceous plant.

Additional components related to iron homeostasis have been characterized. Although not related to mineral uptake, these components are probably involved in iron intracellular targeting and storage. Members of the widely distributed NRAMP (Natural Resistance-Associated Macrophage Protein) family of cation transporters have also been characterized in *Arabidopsis* and rice (Belouchi *et al.*, 1997). *AtNRAMP1, 3* and *4* and *OsNRAMP1* play role in iron homeostasis already exists. *AtNRAMP1* may be related to iron subcellular transport and its targeting to storage compartments in vacuoles or plastids (Curie *et al.*, 2000). Currently, plant genomics allow the fast identification of molecular components related to mineral homeostasis. This is possible through database searches for sequences homologous to proteins already characterized. With this approach, recent reports describe the identification of six genes related to the *NRAMP* family and fifteen genes related to the *ZIP* family in *Arabidopsis* (Maser *et al.*, 2001), as well as eight ORFs with homology to maize *YS1* (Curie *et al.*, 2001).

1.2 Iron storage

Ferritin is an iron storage protein, found in animals, plants, and microorganisms (Theil, 1987; Crichton and Charloteaux-Wauters, 1987). It consists of a mineral core of hydrated ferric oxide; the ferritin protein resembles a spherical shell.

It is made up of 24-protein subunit. This spherical space can be filled up with as many 4500-iron atoms (Caulder and Raymond, 1998). This ferritin protein takes up iron and storage in a non-toxic form, and releases it when needed for metabolic functions. Iron storage in ferritin is bioavailable (Smith, 2004). The ubiquitous iron storage protein ferritin has a highly conserved structure in plants and animals, but a distinct cytological location and different level of control in response to iron excess. In animals the protein is mainly cytoplasmic and there are generally two or more genes that encode closely related subunits (in mammals there are two subunits which are known as H (heavy) and L (light)). These expression mainly controlled at the translation level occurs through the iron-responsive element/iron responsive protein (IRE/IRP) system. In contrast, plants ferritins are plastid–localized and transcriptionally regulated in response to iron (Lobreaux *et al.,* 1993).

In plants, iron-storage protein ferritins accumulate in plastids during seed formation, and also in leaves during senescence or iron overload. Iron release from ferritins occurs during growth of seedlings and the greening of plastids. Overexpression of ferritin in plants results in an increase of resistance to abiotic and biotic oxidative stresses. The multimeric ferritin proteins have been found to maintain cell wall composition (Laulhere and Briat, 1993). For Rice ferritins, there were organized as eight exons and seven introns, located on chromosome 11 and 12 (KOME Report Search, 2004). The evidence supporting ferritin as the major storage protein of iron came from the study using transgenic rice expressing soybean ferritin gene driven by endosperm-specific glutelin promoter. This study was found, the iron content in rice grain doubled in transgenic rice as compared to the non-transgenic control (Vasconcelos *et al*., 2003).

Frataxin: Another protein that plays an important role in iron storage is the frataxin homologue, which has been implicated in iron transport. The frataxin-like domain is related to the globular C-terminus of frataxin, the protein that is mutated in Friedreich's ataxia (Gibson *et al.,* 1996). Mitochondrial processing peptidases and iron homeostasis shown that the mitochondrial intermediate peptidase (MIP) cooperates functionally with frataxin to maintain mitochondrial iron homeostasis in *S.*

cerevisiae (Branda *et al.*, 1999) and that a similar interaction may also exist in mammalian cells (Chew *et al.*, 2000). Yeast frataxin maintains mitochondrial iron homeostasis (i) direct, by promoting iron export and (ii) indirectly, by regulating MIP activity, which stimulates mitochondrial iron uptake. The frataxin homolog from Arabidopsis thaliana (*AtFH*) is a single nuclear-encoded gene targeted to mitochondria and sharing 65% similarity with animal frataxin. The *AtFH* gene knocked out was affected embryo development at the globular stage. Consistent with that, we also show by in situ hybridization that *AtFH* is expressed, in wt Arabidopsis plants, in ovule primordia as well as in embryos at various stages of development, suggesting a key role of plant frataxin during embryogenesis **(**Vazzola *et al*, 2007).

Plant ferritins reside in the chloroplast and are synthesized as larger precursors that are also processed in two steps. Much like two-step processing of frataxin, the functional significance of two-step processing of plant ferritin is unknown. However, in the case of plant ferritin the first cleavage occurs upon import into the chloroplast, while the second takes place after ferritin assembly and has been observed during germination, *in vivo*, and during iron release, *in vitro*. It is possible that two-step processing regulates assembly/iron storage by frataxin (Isaya, 2004).

2. Iron Bioavailability

The low amount of bioavailable iron found in the major staple plant foods (rice, wheat, maize, beans, potatoes, and cassava) is a major contribution factor for iron deficiency in the developing world (Lucca *et al.*, 2001). Increasing the density of iron in plant foods is not enough for solving iron deficiency anemia (IDA), because the bioavailable of Fe in these plant foods. In a case of bioavailable iron, not only must the absolute amounts of iron be increased in the edible portions of these food crops, but also the bioavailable forms of Fe that can consume in typical meals by human.

Iron is one of the abundant elements in the earth's crust. However, it seems that all livings including animals and plants apparently have difficulty absorbing iron

from their environment. Iron absorption refers to the amount of dietary iron that your body obtains from food. Healthy adults absorb about 15% of the iron in their diet, but your actual absorption is influenced by your body's iron stores, the type of iron in the diet, and by other dietary factors that enhance or inhibit iron absorption (Tresca, 2004).

Dietary iron is composed of two forms, heme and non-heme iron. Heme iron, found primarily in meats and animal food, is the most available form of absorption (Haas, n.d.). It is taken up directly by the intestinal cell and within the cell and the iron is enzymatically released from the heme-proteins (Small, 2004). Non-heme iron, found in cereal, legume, green vegetables, etc., is bound to organic constituents of the food. Cooking tends to break these interactions and increase iron availability. At physiological level non-heme iron absorption is mediated by a series of receptors and binding proteins. Heme iron is more easily absorbed than non-heme iron (Rice *et al.*, 1996).

Most of the iron is in the ferric (+++) form and are complexes to other organic and inorganic molecules (Rice *et al.*, 1996; Vance, 2002). The acidity in the stomach and hydrolytic enzymes in the small intestine were released complexes iron. It is then reduced to the ferrous (++) form as it is more readily absorbed. These substances aid the absorption process by either reducing ferric iron to the ferrous state or by mediating iron binding to the mucosal cell receptors. The positive effects of vitamin C are well recognized and widely used in iron fortifications.

Bioavailability of non-heme iron is greatly influenced by both dietary inhibitors and enhancers (Hallberg *et al.*, 1989). This may place certain segments of the vegetarian population that risk for iron deficiency. The balance between absorption facilitators and inhibitors, along with the existing iron status of the individual, determines the bioavailability of iron from individual foods or from a meal (Cheryan, 1980; Kelsay *et al.*, 1988; Hurrell *et al.*, 1992). Amino acids (especially cysteine), ascorbic acid, citric acid, beta-carotene and fructose can enhance iron

absorption, while some organic compounds include phytate, polyphenols, oxalate, tannin, and calcium can inhibit the iron absorption (Tuntawiroon *et al.*, 1991).

3. Iron toxicity

Iron (Fe) toxicity is a major stress in rice in many lowland environments worldwide. Due to excessive uptake of Fe^{2+} by the roots and its acropetal translocation into the leaves, toxic oxygen radicals may form and damage cell. The typical visual symptom is the "Bronzing" of the rice leaves, leading to substantial yield losses, particularly when toxicity occurs during early vegetative growth stages. The problem is best addressed through genotype improvement, *i.e.* tolerant cultivars, etc. (Asch, *et al.*, 2005).

Forward genetic approach for identifying Fe toxicity tolerance mutants. A number of resistance strategies to Fe toxicity in rice have been proposed: (1) Exclusion of Fe^{2+} at the root level, thus avoiding Fe^{2+} damage to the shoot tissue *via* rhizospheric oxidation and root ion selectivity (Chen *et al.*, 1980a, b), (2) inclusion and avoidance *via* internal compartmentation of Fe^{2+} e.g. apoplastic immobilization or preferential storage in old leaves or photosynthetically less active leaf sheath tissue (Audebert and Sahrawat, 2000), and (3) inclusion and tolerance *via* increased thresholds to elevated levels of Fe^{2+} within leaf cells, probably through enzymatic detoxification in the symplast (Thongbai and Goodmann, 2000). One such limiting factor of high grain iron rice breeding is related to the variation in Fe toxicity condition. Most of high iron rice cultivars from natural variation are susceptible to Fe toxic.

4. Iron biofortification in rice

To solve the problem of iron-deficiency anemia, one of the most prevalent human micronutrient deficiencies worldwide, iron-biofortified rice was produced using transgenic approaches. Based on knowledge of Fe transportation and Fe homeostasis in rice, three approaches have been reported to produce Fe-biofortified

rice. The first approach by Goto *et al*. (1999) generated transgenic rice plants that expressed the soybean *ferritin* gene (*SoyferH1*) in the endosperm using the endosperm-specific 1.3-kb *GluB1* rice promoter. The transformants showed higher Fe accumulation in brown rice seeds. The second approach involves increasing Fe transportation within the plant body by enhancing the expression of *NAS* genes. Takahashi *et al*. (2003) was reported suggest that NA plays an essential role in Fe translocation to seeds. In addition, overexpression of the barley *NAS* gene, *HvNAS1*, led to increased Fe and Zn concentrations in the leaves, flowers, and seeds of tobacco plants (Takahashi *et al*., 2003). Likewise, overexpression of the NA synthase gene increased 3 fold Fe concentration in polished rice seeds (Masuda *et al*., 2009; Lee *et al*., 2009 and Alexander *et al*., 2011). The third approach is enhanced of Fe flux into the endosperm by expression of the Fe (II)-NA transporter gene *OsYSL2*. Koike *et al* (2004) identified the rice NA-Fe(II) transporter gene *OsYSL2*, which is preferentially expressed in leaf phloem cells, the vascular bundles of flowers, and developing seeds, suggesting a role in internal Fe transport (Koike *et al*, 2004). *OsYSL2* knockdown mutant plants exhibit a 30% decrease in Fe concentration in the endosperm (Ishimaru *et al*, 2010). In contrast, enhancement of *OsYSL2* expression under the control of the rice sucrose transporter promoter *OsSUT1*, which drives high expression in the panicle and immature seeds during the seed maturation stage, increased Fe concentration in polished rice seeds by up to threefold (Ishimaru *et al*, 2010).

Masuda *et al.* (2012) was produced iron-biofortified rice introduction of multiple genes involved in iron nutrition. Three transgenic approaches were included Enhancing iron storage in grains via expression of the iron storage protein ferritin using endosperm-specific promoters, enhancing iron translocation through overproduction of the natural metal chelator nicotianamine, and enhancing iron flux into the endosperm by means of iron (II)-nicotianamine transporter *OsYSL2* expression under the control of an endosperm-specific promoter and sucrose transporter promoter. The results indicate that the iron concentration of greenhouse-grown T_2 polished seeds was six-fold higher and that in paddy field-grown T_3 polished seeds was 4.4-fold higher than a non-transgenic with no defect in yield. Moreover, the transgenic seeds accumulated zinc up to 1.6-times in the field. This

experiment suggests that, introduction of multiple iron homeostasis genes is more effective for iron biofortification than the single introduction of individual genes.

5. Mutagenesis

One of the most direct ways of establishing gene function is to identify a mutation in the specific gene and to link this mutation to the phenotypic change in the mutated organism. In the forward genetics approach (mutation through phenotype to the gene), large mutated populations have been created and screened for alterations in the trait or biological process of interest. Over the decades, large mutant collections have been developed for many model organisms. These isolated mutants have then served in the identification of the genes underlying the change in phenotype. The sequence of the gene responsible for the altered phenotype can be isolated using the process of map-based cloning. Although this approach is both time-consuming and labor-intensive, it has been successfully applied for cloning several genes, even in species with large genomes, such as barley and wheat (Keller *et al.*, 2005; Komatsuda *et al.*, 2007; Krattinger *et al.*, 2009; Zhang *et al.*, 2009).

Recently large-scale genome sequencing projects have opened up new possibilities for the application of mutation techniques in basic studies and in the improvement of crops. The reverse genetics strategy (gene sequence to phenotype) has widely replaced the forward approach in studies involved in detecting gene function. This strategy is based on the alteration of a gene structure, followed by an analysis of the associated change in plant phenotype. Several reverse genetic technologies, such as insertional mutagenesis with TDNA, transposon tagging or gene silencing, have been proposed for plant functional genomics (Small 2007; Hirochika 2010; Bolle *et al.*, 2011; Upadhyaya *et al.*, 2011). However, the majority of these methods are fully applicable only to model plants with small genomes, such as Arabidopsis or rice, and even in these species, there are some drawbacks that limit their utilization.

TILLING (Targeting Induced Local Lesions IN Genomes) was developed a decade ago as an alternative to insertional mutagenesis in Arabidopsis thaliana (McCallum *et al.,* 2000). TILLING takes advantage of classical mutagenesis, sequence availability and high-throughput screening for nucleotide polymorphisms in a targeted sequence. It combines the high frequency of mutations induced by traditional mutagenesis with sensitive techniques for discovering single nucleotide mutations. The main advantage of TILLING as a reverse genetics strategy is that it can be applied to any plant species, regardless of its genome size, ploidy level or method of propagation. Chemical mutagens, which are usually used in TILLING protocols, provide a high frequency of point mutations distributed randomly in the genome. An analysis of mutations induced by ethyl methanesulphonate (EMS) in 192 Arabidopsis genes revealed about ten mutations per gene among the 3,000 M_2 plants examined (Greene *et al.,* 2003). It was estimated that each M_2 plant carried, on average, 720 mutations (Till *et al.,* 2003), while only 1.5 T-DNA insertions per mutant line were detected in the Arabidopsis insertion populations (Alonso *et al.,* 2003). Thus, much smaller populations are required to reach saturation mutagenesis using TILLING. Five thousand M_1 plants in Arabidopsis (Østergaard and Yanofsky 2004) as compared to 360,000 lines in T-DNA mutagenesis (Alonso and Ecker 2006). The application of TILLING makes the functional analysis of large genomes as well as small genes, which are difficult targets for insertional mutagenesis, possible (Kurowska *et al*., 2011).

Reverse genetics by fast neutron mutagenesis in higher plants. A combining fast neutron mutagenesis and high throughput PCR screening, a new knockout methodology, Deleteagene (Delete-a-gene) was developed in Arabidopsis and rice to obtain deletion mutants for target genes. Since the fast neutron is a highly efficient mutagen that produces deletion mutations easily detectable by PCR, this method has the potential to enable reverse genetic screens in most plant species. The number of plants required to give the same mutation coverage is comparable in plants with different genome sizes.

In some plant species such as Arabidopsis, tomato, and rice, there are sufficient mutagenesis data from the literature that can be used to determine which dose should be used (Ververk, 1959; Yu and Yeager, 1960; Koornneef *et al.,* 1982; Li *et al.,* 2001). For example, 60 Gy is usually used in Arabidopsis and 18-25 Gy is used in rice. Wu *et al.* (2005) produced a large collection of chemical and irradiation-induced IR64 mutants with different genetic lesions that are amenable to both forward and reverse genetics. About 60,000 IR64 mutants have been generated by mutagenesis using chemicals (diepoxybutane and ethylmethanesulfonate) and irradiation (fast neutron and gamma ray). More than 38,000 independent lines have been advanced to M_4 generation enabling evaluation of quantitative traits by replicating trials. Morphological variations at vegetative and reproductive stages, including plant architecture, pigmentation and various physiological characters, are commonly observed in the four mutagenized populations. Conditional mutants such as gain or loss of resistance to blast, bacterial blight, and tungro disease have been identified at frequencies ranging from 0.01% to 0.1%. Results from pilot experiments indicate that the mutant collections are suitable for reverse genetics through PCR-detection of deletions and TILLING. Furthermore, deletions can be detected using oligomer chips suggesting a general technique to pinpoint deletions when genome-wide oligomer chips are broadly available.

6. Nutrition analysis

6.1 Perls' Prussian blue

Perls' Prussian blue staining has been recommended as a method for locating Fe (III) in animal tissue because it is fast, reproducible and the reagent penetrates bulky tissue to give a distinctive blue reaction (Baker, 1958). The technique has recently been used to report the presence of iron in the aleurone layer of rice grain and within part of the seed and across varieties (Prom-u-thai *et al.,* 2003). The principle of this technique including the reaction between ferric iron deposits in tissue (present mostly as ferric iron within the storage protein ferritin) and soluble

ferrocyanide in the stain, to form an insoluble Prussian blue dye in situ. They are then visualizable microscopically as blue or purple deposits, within cells.

6.2 Atomic Absorption Spectrophotometer

Atomic absorption spectrometry (AAS) is a spectro analytical procedure for the quantitative determination of chemical elements employing the absorption of optical radiation (light) by free atoms in the gaseous state. Atomic absorption is so sensitive that it can measure down to parts per billion of a gram (μg dm^{-3}) in a sample. The technique makes use of the wavelengths of light specifically absorbed by an element. They correspond to the energies needed to promote electrons from one energy level to another, higher, energy level. Atomic absorption spectrometry has many uses in different areas of chemistry in analytical chemistry the technique is used for determining the concentration of a particular element in a sample to be analyzed. AAS can be used to determine over 70 different elements in solution or directly in solid samples employed in pharmacology, biophysics and toxicology research (Welz and Sperling, 1999).

6.3 Inductively coupled plasma (ICP)

Inductively coupled plasma atomic emission spectroscopy and inductively coupled plasma mass spectrometry (ICP-AES and ICP-MS) are a technique for elemental analysis, used for bulk elemental chemical analysis of just about any material or substance (waters, biological materials, inorganic materials, environmental samples, geological samples, etc.). Most of the periodic table (with the exceptions of H, O, N, F, Cl, Br, I) can be measured using ICP-AES and ICP-MS. Concentrations from major to parts per billion or in many cases parts per trillion in solutions can be measured. Both ICP-MS and ICP-AES enable the nondestructive sampling of plants, a boon for large-scale genetic screening. The ICP-MS and ICP-AES technologies are readily available but relatively low resolution of ion detection assays. These methods are appropriate for the reproducible growth and analysis of mutant plants for high-throughput nutrient analysis (Hirschi, 2003).

6.4 Iron bioavailability analysis method: In vitro Digestion/Caco-2 Cell

An *in vitro* "artificial gut" for iron-bioavailability testing in foods and crops is helping make faster and more cost-effective. Artificial gut using Caco-2 cells, which are resemblances to the epithelial cells that line the human small intestine. The model was matched on a relative basis, those effects known to occur in humans. In Glahn's system, Caco-2 cells are placed in the bottom of culture wells, and then covered by a dialysis membrane that functions like the mucus layer that protects human intestinal cells. Food and digestive enzymes are placed on top of the membrane. This prevents the enzymes from reaching the cells, while nutrients and minerals pass through. Next, the amount of ferritin in the Caco-2 cells is measured. Ferritin formation is a highly sensitive and accurate measurement of iron uptake. Finally, comparing the amount of absorbed iron to the amount originally present in the food yields the iron bioavailability for that food. Rice cereal, breast milk, infant formulas and iron supplements were investigated for available iron. This system might also measure bioavailability on the crop level. Researchers could screen varieties of rice, beans, wheat and corn for improved iron availability (Glahn *et al*., 1998).

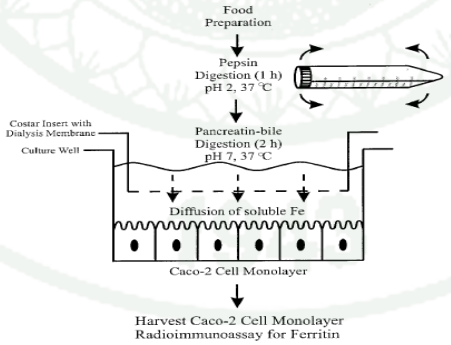

Figure 2 Diagram of in vitro digestion/Caco-2 cell culture model

Source: Glahn *et al.* (1998)

7. Molecular Genetic Analysis

7.1 Denaturing High Performance Liquid Chromatography (DHPLC)

DHPLC is an ion-pair reversed-phase high performance liquid chromatography (IP-RP-HPLC). Denaturing high performance liquid chromatography (DHPLC) is an introduced high-throughput method that facilitates mutation detection of short double stranded DNA molecules (Oefner and Underhill 1998). This method is based on mismatched heteroduplex formation between wild type and mutant DNA single strands. These mismatched heteroduplexes and matched wild type and mutant homoduplexes differ from each other in their thermostability. When separated by means of a chromatography column at a sequence-specific melting temperature and gradient elution buffer (acetonitrile), heteroduplexes and homoduplexes will elute at different times, giving rise to complex chromatograms. Therefore, the presence of a one-peaked chromatogram is evidence of wild-type DNA, whereas complex chromatograms (two or more peaks) indicate the presence of wild type and mutant (Klein *et al.*, 2001). DHPLC is a rapid, highly sensitive and comparatively inexpensive mutation screening technology. It is widely used in molecular genetics diagnostics & SNP research labs.

7.2 Single Feature Polymorphism (SFP)

Single feature polymorphism (SFP) by using DNA-based gene-chip approach to identify polymorphism in rice were demonstrating that hybridization of probes, generated from labeling of g-DNA, to rice whole genome expression array (Affymetrix). SFP is a high-throughput and effective method in genome-wide polymorphism detection. The sensitivity of polymorphism detection was further demonstrated by the fact that no biasness was observed in detecting SFP with either single or multiple nucleotide polymorphisms. The high density SFP data that can be generated quite effectively by the current method has promise for high resolution genetic mapping studies, as physical location of features is well-defined on rice genome (Kumar, *et al*., 2007).

7.3 Next-generation sequencing

Next-Generation Sequencing (NGS), a fundamentally different approach to sequencing that triggered numerous groundbreaking discoveries and ignited a revolution in genomic science. In principle, the concept behind NGS technology is similar to CE. The bases of a small fragment of DNA are sequentially identified from signals emitted as each fragment is re-synthesized from a DNA template strand. NGS extends this process across millions of reactions in a massively parallel fashion, rather than being limited to a single or a few DNA fragments. This advance enables rapid sequencing of large stretches of DNA base pairs spanning entire genomes, with the latest instruments capable of producing hundreds of gigabases of data in a single sequencing run. The newly identified strings of bases, called reads, are then reassembled using a known reference genome as a scaffold (resequencing), or in the absence of a reference genome (de novo sequencing). The full set of aligned reads reveals the entire sequence of each chromosome in the gDNA sample (Illumina, 2013).

7.4 Gene-expression

Gene expression is the most fundamental level at which genotype gives rise to the phenotype. The genetic code is "interpreted" by gene expression, and the properties of the expression products give rise to the organism's phenotype. Expression profiling experiments often involve measuring the relative amount of mRNA expressed in two or more experimental conditions. This is because altered levels of a specific sequence of mRNA suggest a changed need for the protein coded for by the mRNA, perhaps indicating a homeostatic response or a pathological condition.

MATERIALS AND METHODS

Part I: Potential of using natural variation for grain Fe density and bioavailability

1. Plant materials

Segregating populations were developed from crossbreeding. High grain Fe rice parents were selected and crossed to desirable traits otherwise low Fe. Four RIL populations as Homsupan/JHN; KDML105/ JHN; Hompama/ Kum Doi Chang and *O. nivara* / JHN were used in this experiment. Desirable progenies were screened-out by pedigree selection. Marker-assisted selections were established on cooking quality trait. Selected-lines of breeding program were analyzed nutritional profile.

2. Nutritional analysis

Nutritional analysis was conducted at Institute of Nutrition, Mahidol University (INMU). The raw seed was cleaned and washed one time with deionized water at ratio 1:3 in order to remove adhering contaminants for 30 seconds, then the samples were dried in the hot air oven at 60ºC for 6 hours and then ground with an electric coffee grinder. The powdered samples were kept in zip-lock plastic bag. Rice samples were determined the moisture content as follows AOAC, 2000 method. For iron, zinc and copper contents in the samples were determined after wet-digest by conc. nitric/perchloric acid at ratio 5:1 and measured by ICP-OES. Polyphenol, tannin and catechin were determined by following the method of Brune, *et al* (1991). For phytate content was measured as follows the method of Christine Hotz and colleague (2001).

3. Iron bioavailability

The bioavailability of iron in new breeding lines were evaluated by using *in vitr*o digestion Caco-2 cell at INMU. Large numbers of high Fe-dense rice lines were screened-out for metabolic and efficacy trials. The factors that can promote and inhibit the absorption of iron in the body, including amylose, amylopectin, rapidly available glucose, beta-carotene, phytate, proanthocyanin, polyphenol, tannin, etc. were characterized by using a high iron rice progenies from 'Hompama x Kam Doi Chang' population.

4. Yield observation of high nutrition rice on Fe toxic field

Seventeen high nutritional rice and standard varieties were selected for yield observation in the Fe toxic paddy field (acid sulfate soil). Rice grain from tolerance lines were collected for iron density analysis to compare with the harvested grain from the normal pH paddy field.

5. Sequence variation of candidate genes for iron homeostasis

Natural variation varieties differ in iron density and bioavailability were selected for identifying the sequence variation on major candidate genes for iron homeostasis such as two iron storage protein, ferritin (*OsFer1* and *OsFer2*). Gene-specific markers were designed based on genomic sequence available at MSU (http://rice.plantbiology.msu.edu) and Gramene (www.gramene.org). PCR primers were designed by using Primer3 software coverage 5'UTR to 3' UTR of the gene sequence. The PCR fragment from each primer is range in 500-700 bp. After amplification, PCR amplicons were sequenced by using direct-sequencing (Applied Biosystems) and assembly a contigs by using CAP3 Sequence Assembly Program.

Part II: Identification of mutant lines conferring high grain Fe density and tolerance to Fe toxicity

1. Plant materials

Mutation library was constructed by using Jao Hom Nin (JHN), a purple nutritious rice developed in Thailand. About 100,000 JHN breeder seeds were mutagenized by using 33 Gy fast neutrons (FN) at the Office of Atoms for Peace (OAP), Thailand. Treated seeds were directly sown in soil in the field to produce M_2 seeds. Eight M_2 plants (represent the M_1 family) were grown in the field to advance to the next generation.

2. Forward genetics screening

Forward genetic approach was used for identifying high/low grain iron density and iron toxicity tolerance mutant in M_4 population. In order to screen for high iron mutants, two approaches were 1) iron density screening in brown rice by using modified Perl Prussian blue method and 2) seedling screening under Fe toxic nutrient solution (300 ppm FeEDTA).

2.1 Grain iron density

2.1.1 Rapidly Screening: Modified Perl's Prussian Blue (PPB)

High and low grain Fe density mutants were isolated by mass screening of 12,000 M_4 lines (5 seeds per lines) using Modified Perl's Prussian Blue (PPB) from Prom-U-thai *et al* (2003) by removing pericarp and embryo color with 6 % sodium hypochlorite for 20 minutes before an experiment. Rice grains were imbibed in distilled water for 4-5 h. Then, cut the grain in haft lengthwise (longitudinal) through the embryo with a knife. Submerged the grain in freshly prepared staining solution (2% potassium ferrocyanide + 2% hydrochloric acid) for 30 min. Washed continuously in distilled water for 2 minutes, 2 times. Estimated the

intensity of staining intensity on rice grain (especially embryo and pericarp) by comparing with standard varieties. A standard checks for PPB score were included the high grain Fe variety (IR68144 (Score++: 17 ppm Fe)), low grain Fe (KDML105 (Score 0: 10 ppm Fe)) and JHN wild type with intermediate Fe (Score+ 13 ppm Fe).

2.1.2 Standard technique: AAS and ICP-OES

Brown rice samples including standard varieties, selected-progenies lines from crossbreeding population and iron density mutant lines by PPB screening were analyzed for grain iron content using AAS and ICP method. Twenty grams of cleaned-rice grains were ground and determined for moisture content. Rice flour was digested with conc. nitric/perchloric acid at ratio 5:1 overnight in a fume hood. Since, digestion this sample in the hot air oven (120$\pm$5 °C) for 6-8 h until the solution was clear. To determine the iron content by using atomic absorption spectroscopy (AAS) and/or inductively coupled plasma mass spectrometry (ICP-OES).

2.2 Iron toxicity

Fe toxicity tolerance screening was initiated from ten-day old M_4 seedlings. Ten plants per line of mutants were grown under low pH nutrient solution with excess available iron (pH 3.0, FeEDTA 300 ppm). Tolerance and susceptible phenotype were characterized based on leaf bronzing index measurement followed by Arbelt (2003) protocol **(Figure 3**) until JHN wild type died. The localization of iron in various part of the leaf was determined by PPB.

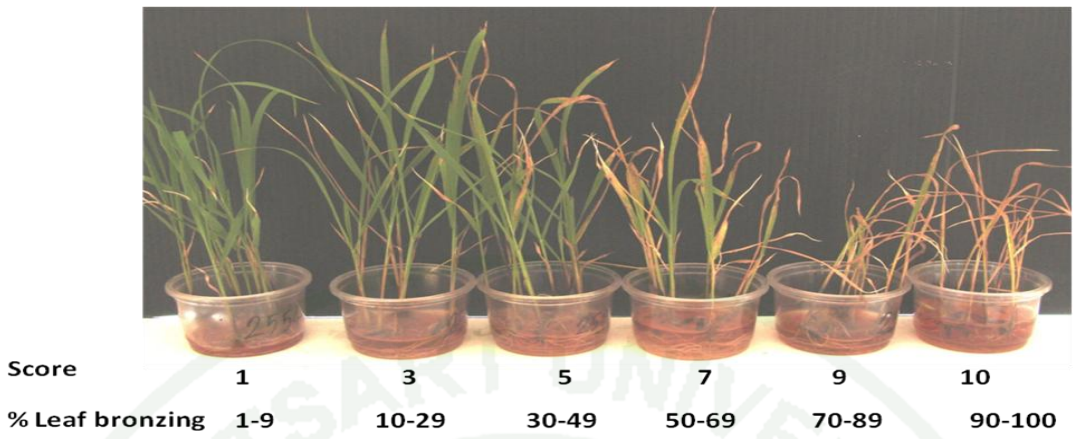

Figure 3 Percent leaf bronzing and scoring rate of rice seedling under Fe toxic treatment (300 ppm FeEDTA, pH3.0)

3. Reverse screening

For reverse genetics, the general protocol for the creation of a TILLING platform in plants was included the DNA extraction and mutation detection on target genes for iron homeostasis.

3.1 DNA Extraction

Young leave from the M_2 and M_4 plants were collected for genomic DNA extraction by CTAB method. Twenty-four leaf pieces with the same size and weight that represent 24 mutant lines were pooled in 1 dimension (1D) before the DNA extraction.

3.2 Primer design

Gene-specific markers were designed based on coding sequence of important iron homeostasis gene available at MSU (http://rice.plantbiology.msu.edu) and Gramene (www.gramene.org). The target size of PCR fragment is range in 500-700 bp (appropriate for DHPLC and DNA sequencing method).

3.3 Polymerase chain reaction PCR

Total 24,000 M_2 were PCR screened using gene–specific primers designed based on coding sequence of 6 candidate genes as *OsFRO1, OsFer1, OsFer2, OsIRT1, OsNAS3 and OsYSL1.* PCR reactions were performed using a KAPA2G^{TM} Robust HotStart PCR kit (Kapa Biosystems, Boston, MA, USA) in 20 µl reaction mixture consisting of 4 µl of KAPA2G Buffer A (containing 1.5 mM $MgCl_2$), 0.4 µl of 20 mM $MgCl_2$, 0.4 µl dNTP (10 mM), 0.08 µl KAPA2G Robust DNA polymerase (5 units/µl), 12.32 µl sterilized distilled water, 0.4 µl of each 5 µM forward and reverse primers, and 2 µl genomic DNA (50 ng) as template. The PCR was performed in a 96-well GeneAmp® PCR System 9700 thermal cycler (Applied Biosystems, Foster City, CA, USA). After preheating at 95 °C for 3 min, the PCR reaction was carried out for 35 cycles under the following conditions: denaturing at 95 °C for 30 s, annealing at 55 °C for 30 s and extension at 72 °C for 30 s, followed by one cycle at 72 °C for 2 min at the end of amplification. After the thermal cycle, PCR products were checked on 1.5-% agarose before use in the next experiment.

3.4 Denaturing high performance liquid chromatography (DHPLC)

After PCR amplification, products were denatured at 95 °C for 5 min and slow annealed step from 95 °C to 65 °C over 30 min to promote heteroduplexes before analyzed by DHPLC undertaken on the Varian Helix system controlled by Star Reviewer software. The recommended temperatures for running of each amplicons were predicted by the melting algorithm available at http://insertion.stanford.edu/melt.html. The Varian Helix system comes with two validation standards: pUC18 and DYS271. The analyses of both standards are crucial to ensuring optimal system performance. Before running the sample, detect non-specific products resulting from mispriming and /or primer-dimer formation by analyzing homo and heterozygous samples in a non-denaturing temperature (50 °C). For sample running, only one temperature was changed depends on sequence descriptions of each fragment at 50-70 °C, but the gradient and flow rates was conducted in the same manner. DHPLC chromatograms from a DNA pool that show

addition peak more than JNH wild type may contain mutants. A mutant line on positive pool was characterized by individual plant screening followed these steps.

3.5 DNA Sequencing

One representative mutation amplicons were confirmed by direct-sequencing (Applied Biosystems). The sequencing method was conducted by using automate sequencer. Fluorescent dye labels incorporated into DNA extension products using 3' dye labeled dideoxynueclotide triphosphates (dye terminator). DNA sequencers detect fluorescent from four different dyes that used to identify the A, C, G and T extension reaction. Each dye emits light at a different wavelength when excited by an argon ion laser. All four colors and therefore all four bases can be detected and distinguished in a single lane. The sequence results from JHN wild type and mutants were analyzed by using Clustal W software to determine a sequence variation.

3.6 Characterization of candidate genes mutant

To understand the function of candidate gene mutants, identified mutant line was evaluated on the related phenotype including grain Fe density and plant adaptation under Fe toxic nutrient solution by comparing with JHN wild type.

3.7 Development of gene-specific markers for MAS

Sequence variations in characterizing genes were generated for gene-specific markers. These markers were surveyed on rice germplasm and mutant population.

Part III: Identification of candidate genes for grain Fe density

1. Plant materials

In order to rapidly identify mutations by forward screening, two extremely mutants for grain iron were applied to survey genome-wide mutation by SFP. The highest grain Fe density mutant (Mu4643) contains 29 ppm Fe while, the lowest mutant (Mu8097) contains only 7 ppm grain Fe.

2. Genome-wide mutation screening

Genomic DNA from 2 different lines including highest and lowest mutant lines were used for single-feature polymorphism (SFP) mapping comparing the genomic DNA of JHN wild type. Genome-wide screened for SFP was conducted using 57K Rice GeneChip expression array which build 11 feature probes on every annotated genes in rice. There are 48,564 genes from japonica and 1,260 genes from indica (each gene composes with 11 probes in 25 bp length) were spotted on Affymetrix Genechip. SFP mapping was performed following the protocol developed by Kumar et al. 2007. No significant variation between samples or replicates was observed. A statistical analysis of the microarrays was performed, and SFPs were predicted by determining the hybridization differences at each perfect match (PM) probe in the array (Thongjuea *et al.*, 2009). Significant probe/features were identified at a false discovery rate of 30%.

3. SFP confirmation by direct sequencing

A total of 4 predicted iron homeostasis related-SFPs in low grain Fe mutant (Mu8097) were validated by direct sequencing on the predicted variable location on the genome. To identify SNPs and indel on mutant lines by comparing with JHN.

4. Expression analysis of SFP-related genes

Total RNA from various developing stages of rice plant were extracted using TRIZOL. RT-PCR was performed by using QIAGEN OneStep RT-PCR standard protocol (QIAGEN OneStep RT-PCR Kit Handbook, 2008). The total volume 25 ul including 10 ul of RNAse-free water, 5 ul of 5X QIAGEN OneStep RT-PCR Buffer, 1ul of 10mM dNTPsMix, 3 ul of each 5uM F_Primer and R_Primer, 1 ul of OneStep RT-PCR enzyme and 50 ng/ul and 2 ul of 50 ng/ ul RNA template. The PCR was performed in a 96-well GeneAmp® PCR System 9700 thermal cycler (Applied Biosystems, Foster City, CA, USA). The reverse transcription step was synthesized at 50 °C for 30 min and 95 °C for 15 min. After reverse transcription, PCR reaction was carried out for 25-35 cycles under the following conditions: denaturing at 94 °C for 30 s, annealing at 50-60 °C for 30 s and extension at 72 °C for 1 min, followed by one cycle at 72 °C for 2 min at the end of amplification. The control gene expression was housekeeping gene "beta-actin" or ubiquitin. After the thermal cycle, RT-PCR products were checked on 1.5-% agarose.

5. Genomic characterization of SFP-related genes

The SFP-containing genes were classified based on the sequence variations between JHN and mutant. Furthermore, protein translation and domain identification on mutant line was analyzed for understanding the effect of induced mutation**.**

RESULTS AND DISCUSSION

Results

Part I: Potential of using natural variation for grain Fe density and bioavailability

1. Distribution of grain iron density

On the breeding activities, the extensive survey of iron density among landraces identified potential donors of high iron density. The majority of these high iron rice lines belong to the black purple rice. The major limitation to using these rice germplasm is high inhibition factors for bioavailabity as tannin, polyphenol and phytic acid contents in the rice bran. Because white color rice is low in those inhibition factors, attempts were made to hybridize white x purple rice parents to transmit high iron density to normal white rice.

The distribution of grain iron density for 4 crosses indicated that iron ranged from 1.0-1.5 mg/100g in SP/JHN, 1.5-2.1 in KDML105/JHN, 2.0-2.8 in HPM/KDC and more than 3 mg/100g in *O.nivara*/JHN cross **(Figure 4)**. The first successful white rice from KDML105/JHN cross contains 2.1 mg / 100 g as the whole grain. This pure line called for 'Sinlek' is aromatic with intermediate amylose content. From crosses between upland rice, Kum Doi Chang (KDC) and Hom Pamah, we successfully identified white color rice with 2.8 mg/100 g of grain iron. The high iron density line was identified as progenies from the hybridization between a wild rice, *O. nivara* and high iron rice Jao Hom Nin (JHN). One of the highest iron dense rice contained up to 4.95 mg/100 g. Our emphasis is now directed to improving iron bioavailability.

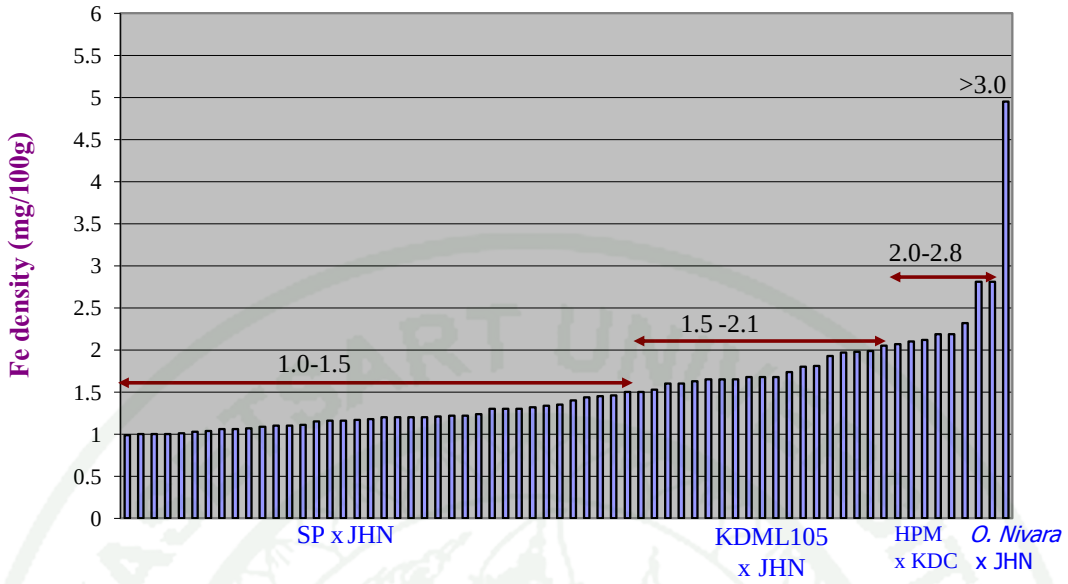

Figure 4 Distribution of Fe density (mg/100g) in Four RIL populations as Homsupan/JHN; KDML105/ JHN; Hompama/ Kum Doi Chang and *O. nivara* / JHN

2. Iron bioavailability

For the natural inhibitors to iron absorption, polyphenol, condensed tannin and phytic acid are the most potent inhibitors of iron absorption. Reduction of these natural inhibitors was the primary objective in cross-breed new strains of white color rice. The iron bioavailability analysis by using Caco-2 cell on 12 selected lines from the model population 'Hompama x Kam Doi Chang' found that total phytate (Inositol pentaphosphate: IP5 + Inositol Hexaphosphate: IP6) and zinc content were negatively correlated to an iron bioavailability (**Figure 5)**. This result was confirmed by the iron bioavailability on 32 high nutritional lines from NRCT project **(Appendix Table 1)**. Thus, improvement of high iron bioavailability rice should be reduced total grain phytic acid content.

	Beta	color	FeBio	Fe	Lutein	Phytate	Polyphenol	tannin
Color	.7764 (12) . 30							
FeBio	--.1673 (12) .6033	--.2153 (12) .5016						
Fe	.1065 (12) .7418	- .-190 (12) .9534	- .-870 (12) .7880					
Lutein	. 212 (12) .9478	.3475 (12) .2684	- .-428 (12) .8949	.1255 (12) .6976				
Phytate	. 156 (12) .9615	- .-453 (12) .8889	--.8000 (12) . 18	. 303 (12) .9255	--.3140 (12) .3203			
Polyphenol	.7560 (12) . 44	.9894 (12) . 0	--.2309 (12) .4703	- .-865 (12) .7892	.4047 (12) .1919	- .-735 (12) .8204		
Tannin	.8938 (12) . 1	.8923 (12) . 1	--.1257 (12) .6970	. 325 (12) .9201	.2605 (12) .4134	- .-266 (12) .9347	.8586 (12) . 3	
Zn	.3149 (12) .3188	.1787 (12) .5784	--.7848 (12) . 25	.2964 (12) .3495	- .-901 (12) .7807	.6376 (12) . 257	.1660 (12) .6061	.1393 (12) .6659

Correlation
(Sample Size)
P-Value

Figure 5 Correlation between seed color, iron, zinc, beta-carotene, lutein, phytate, tannin, and polyphenol content on iron bioavailability (Fe Bio) among selected lines from cross 'Hompama x Kam Doi Chang'

3. Yield observation of high nutrition rice on Fe toxic field (acid sulfate soil)

Seventeen high nutritional rice cultivars were selected for yield observation in the Fe toxic field (acid sulfate soil) with contain 234 mg/kg Extr.Fe, pH 3.57 at Nakhonnayok (NN). The limitation to increase grain Fe density is that most rice is susceptible to Fe toxicity **(Table 1).** In this experiment, there were two breeding lines from KD/JHN cross pedigree No. 909-10-1-3 and 909-21-2-5 had highly percent of plant survival under Fe toxic condition and can accumulated 35.5 and 39.8 % more Fe in the grain respectively, as compared to harvested seeds under neutral pH conditions in KPS KU.

Table 1 Percent plant survival of 17 high nutritional lines grown on iron toxicity field with contains 234 mg/kg Extr. Fe, pH 3.57

No.	Varieties	% Survival			
		Rep I	**Rep II**	**Rep III**	**Rep IV**
1	Pinkaset	10	0	<5	5
2	Jao Hom Nin	<5	<5	40	0
3	IR68144	0	0	5	<5
4	BW1	10	50	20	<5
5	Sinlek	5	15	60	15
6	Riceberry	15	20	10	10
7	*O. nivara* x JHN#91	50	10	60	<5
8	*O. nivara* x JHN#299	5	20	20	10
9	KDxJHN# 909-21-2-5	90	85	95	10
10	KDxJHN#909-10-1-3	85	20	85	15
11	KDxNHN#629-44-1	10	30	10	30
12	SPxJHN#49-36	40	10	15	10
13	IR71501 x Pinkaset #3-1-22-6-1	30	0	20	5
14	IR71501 x Pinkaset #34-1-3-1-0	10	5	20	5
15	KDCxHPM#18-3-17-1-11-0	<5	<5	0	0
16	KDCxHPM#49-6-6-1-1-0	0	0	5	5
17	KDCxHPM#31-9-11-1-0	5	<5	<5	0

Table 2 Total iron, zinc and copper content in brown rice grain harvested from different fields (KPS and NN)

Name	Fe (mg/kg)		Increased (%)	Zn (mg/kg)		Increased (%)	Cu (mg/kg)		Increased (%)
	KPS	NN		KPS	NN		KPS	NN	
KD/JHN 909-10-1-3	9.3	12.6	35.5	26.7	42.3	58.4	1.7	5.4	217.6
KD/JHN 909-21-2-5	8.3	11.6	39.8	21.2	41.7	96.7	1.8	6.9	283.3

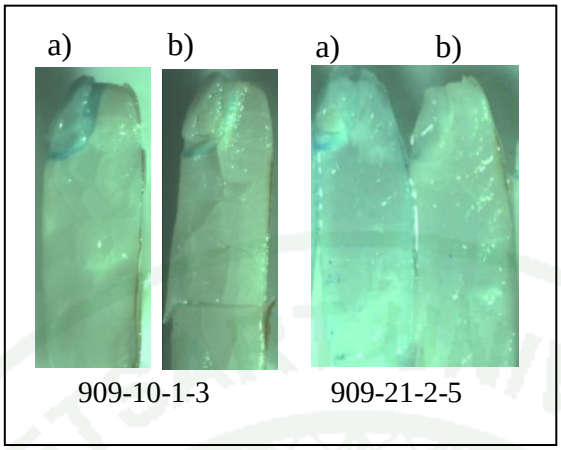

Figure 6 Perl Prussian blue staining intensity on embryo partition of two Fe-toxic tolerant breeding lines harvested from different fields: a) NN and b) KPS KU

5. Sequence variation in ferritin genes

Sequence variation of two ferritin (*OsFer1* and *OsFer2*) was identified based on 7 rice varieties including Xua Bue Nuo (XBN), Jao Hom Nin (JHN), IR68144, Sinin (BT#3), KDML105 (KD), Azucena (Azu) and reference Nipponbare (Nip). Multiple sequence variation (MSA) on *OsFer1* showed that 17 identified SNPs; 12 SNPs located in upstream, 1 was synonymous SNP on exon2, 5 SNPs located on downstream and found 10 bp insertion in promoter sequence. All of SNPs and insertion can divide 7 rice varieties for two groups and related rather than grain iron density. While, *OsFer2* contain 7 identified SNPs; 2 SNPs located in upstream, 1 were synonymous SNP on exon1 and 4 SNPs located on the downstream. However, there were no associated haplotypes on *OsFer2* **(Appendix Table 2)**.

Part II: Identification of mutant lines conferring high grain Fe density and tolerance to Fe toxicity

1. Generating mutant libraries

About 100,000 JHN breeder seeds were mutagenized by using 33 Gy fast neutrons (FN) at the Office of Atoms for Peace, Thailand. Treated seeds were directly sown in soil in the field to produce M_2 seeds. Eight M_2 plants (represent the M_1 family) were grown in a field to advance to the next generation. **(Figure 7)** Up-to-date 21,024 M_5 were maintained in the field. DNA libraries were collected from the M_2 and M_4 plants were collected (24 lines/DNA pool).

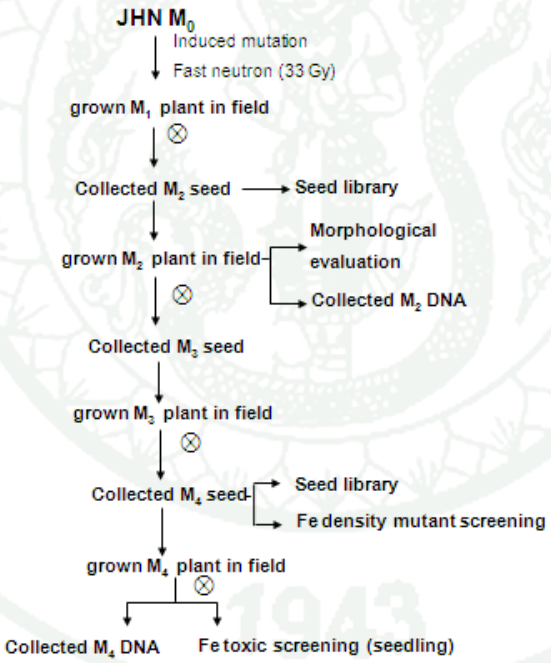

Figure 7 Jao Hom Nin (JHN) mutant population developing flow chart

2. Forward screening for identifying Fe dense and Fe toxicity mutants

The forward genetic screening was used for identifying high/low grain iron density and iron toxicity tolerance mutant in M_4 population. A total of 12,000 M_4

lines was screened for Perl Prussian Blue (PPB). Higher and lower PPB scores when compared to JHN wild type were further analyzed by AAS and ICP. The base mutant population was also screened under Fe toxic (pH 3.0, FeEDTA 300 ppm) nutrient solution at seedling stage **(Figure 8)**.

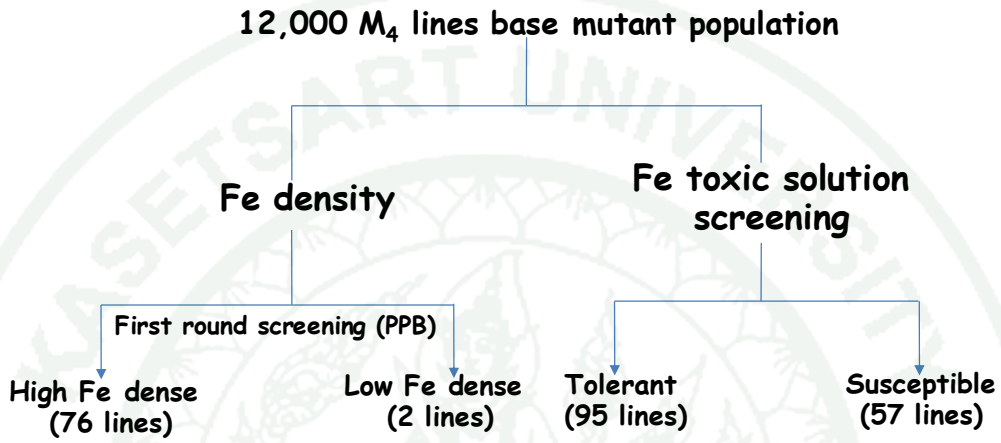

Figure 8 Forward screening flow charts for identifying Fe dense and Fe toxicity mutants. Numbers in parentheses refer to mutant lines in each group of phenotypic screening

2.1 Grain Iron density screening

High and low grain Fe density mutants were isolated by mass screening of 12,000 M_4 lines (5 seeds per lines) using Modified Perl's Prussian Blue (PPB) from Prom-U-thai *et al* (2003). So far, 76 lines contained higher Fe grain density while only two lines contained much lower Fe-content grains than the wild type **(Figure 9)**. The highest grain Fe density was 29 ppm (Mu4643) whereas the lower one contained only 7 ppm (Mu8097). There were global agreement between PPB score and both ICP and AAS methods. The colorimetric PPB allows the most rapid screening method for detecting large variation in Fe-grain density found in embryos and the pericarp of rice grains. Whereas, ICP and AAS are more sensitive and be able to analyze the whole grain including low Fe-density endosperm.

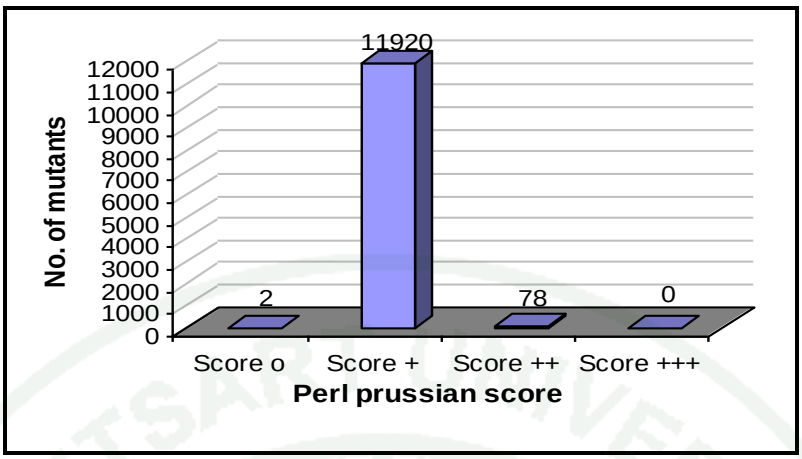

Figure 9 Distribution of Prussian blue staining score for Fe density evaluation of M_4 JHN mutant population

2.2 Fe toxic screening

Fe toxicity tolerance screening was initiated from ten-day old M_4 seedlings (10 plant per line) grown under low pH nutrient solution with excess available iron (pH 3.0, FeEDTA 300 ppm). Among 12,000 M_4 lines being screened, including selected mutants with high and low grain Fe density from PPB screening, we found that 95 and 57 lines were tolerant and susceptible, respectively, when compared to JHN wild type.

3. Phenotypic distribution of grain Fe density and Fe toxicity tolerance

At the Fe toxic screening, we found that the majority (98.5%) show a similar phenotype as JHN. For the 1.5 % mutant group, only 97 M_4 lines contained medium Fe density (M) and Fe toxicity tolerance (T) = MT. While, HM (52 lines) can accumulation iron in rice seeds well in normal soil conditions and moderately resistant to iron toxicity. However, we cannot identify the LT, LS and HT groups from this population. The broadcast group HS found in this population was similar to rice varieties from natural crossbreeding **(Figure 10)**. New mutants would be useful for breeding to be a HM (including Mu4643) and MT (including MuFRO). These

mutants had been a great deal to increase the rice production of iron in soils with iron poisoning.

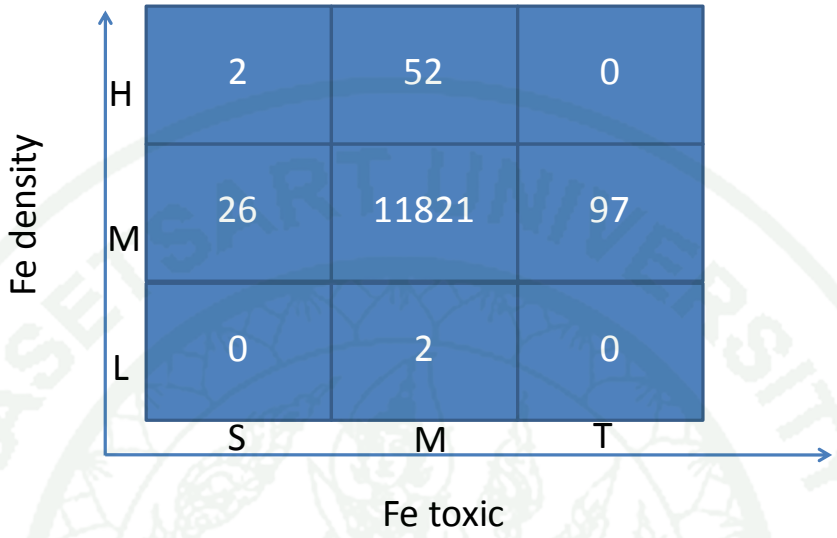

Figure 10 The distribution of 12,000 M_4 lines for the co-expression of grain Fe density and tolerance to Fe toxicity solution. Phenotypic categories including High grain Fe density (H), Medium grain Fe density M) Low grain Fe density (L) Tolerance to Fe toxicity (T) Moderate to Fe toxicity (M) and Susceptible to Fe toxicity (S). There were combined for 9 combinations as H-T, H-M, H-S, M-T, M-M, M-S, L-T, L-M and L-S

4. Screening for sequence variation in candidate genes for iron homeostasis

Although forward screening can identify abundant Fe mutants, but it is essential to survey the mutation on candidate gene sequences. Genomic DNA pools from 24 M_4 plants (represent 1 M_1) of Fe mutants were PCR screened using gene–specific primers designed based on coding sequence of 6 candidate genes as *OsFRO1* (LOC_Os04g36720), *OsFer1* (LOC_Os11g01530), *OsFer2* (LOC_Os12g01530), *OsIRT1*(LOC_Os03g46470), *OsNAS3*(LOC_Os07g48980) and *OsYSL16* (LOC_Os04g45900) (Kawahara *et al.*, 2013). After PCR amplification, products were denatured and slow annealed to promote heteroduplexes before analyzing by DHPLC.

However, we only found that mutation on *OsFRO1* amplicon, but cannot detect in other genes. Among 5 mutant lines was contained *OsFRO1* mutant sequence. One mutant was purified and called for “MuFRO”. Sequence comparison on *OsFRO1* between MuFRO and JHN wild type were identified five Single Nucleotide Polymorphisms (SNPs), one indel and two non-synonymous SNP or Single Amino Acid Polymorphisms (SAP). One of SAPs was located on the Ferric reductase domain (pfam01794, Marchler-Bauer *et al.*, 2011) **(Figure 11).**

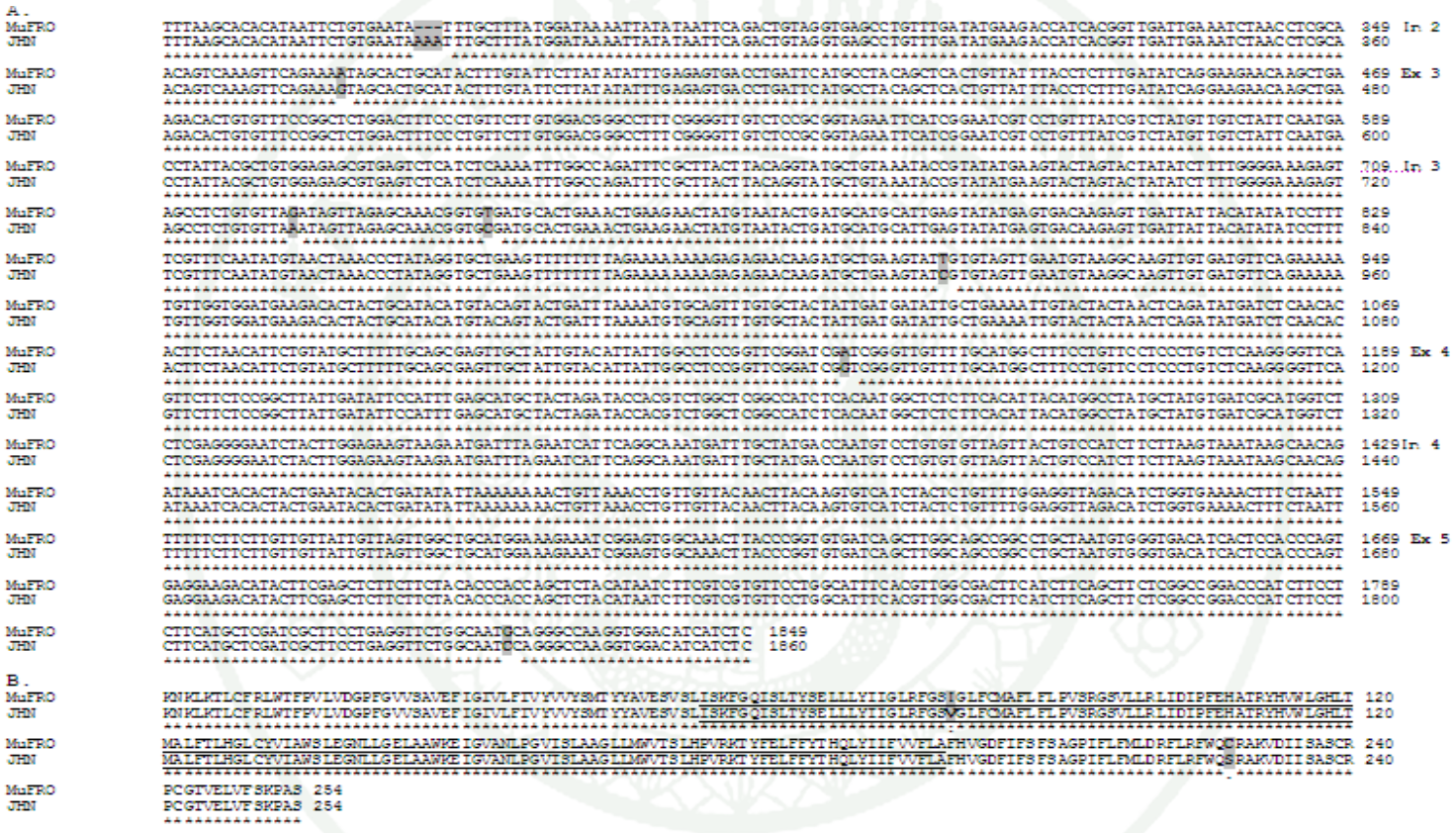

Figure 11 A mutations discovered on Ferric chelate reductase (*OsFRO1*; LOC_Os04g36720) sequence in MuFRO A) nucleotide sequence alignment between intron 2 to exon 5 between JHN wild type and MuFRO and B) Amino Acid sequence alignment represent SAP on exon 4 and 5. The underlined amino acids were represented Ferric_reduct domain [pfam01794]

6. Characterization of *OsFRO1* mutant

OsFRO1 (LOC_Os04g36720) encodes for the enzyme Ferric chelate reductase. It is an ortholog of Arabidopsis Ferric-chelate reducatase gene (*FRO2*) that play a role in iron uptake by plants **(**Robinson *et al.,* 1999 and Einset *et al.,* 2008). *OsFRO1* is expressed in the leaves of Zn-, Mn-, and Cu-deficient rice plants (Ishimaru *et al.,* 2006). RNA sequence coverage of *OsFRO1* available on the MSU Rice Genome Annotation Release 7 shown that *OsFRO1* was highly expressed in various tissues, especially seedling, leaf and early seed development stage. While, *FRO2*-like genes (*OsFRO2*) show only highly transcript in leave (Trapnell *et al.,* 2010). To understand the function of the *OsFRO*1 mutants comparison with JHN wild type. Two specific phenotype including grain Fe content and plant adaptation under Fe toxicity nutrient solution were evaluated**.**

6.1 Grain iron density analysis of MuFRO

JHN and MuFRO seeds harvested from two generations were analyzed for Fe and Zn contents by using ICP-OES at INMU. The result found that both M_3 and M_4 seeds from MuFRO contain 20-30% more grain iron than JHN wild type, **(Table 3)** but there was no change in zinc and contents. The variation of grain iron content between wild type and mutant indicates that *OsFRO1* may affect iron storage capacity of rice grains.

Table 3 Iron and zinc contents in JHN and MuFRO brown rice seeds from two generations

No.	Name	Fe (ppm)	Zn (ppm)
1	MuFRO (M_3 seed)	13.7±0.3	17.7±0.7
2	JHN (control)	10.5±0.3	16.6±1.2
3	MuFRO (M_4 seed)	11.7±0.2	25.8±2.3
4	JHN (control)	9.4±0.2	25.4±1.2

6.2 Effect of iron stress on the growth of MuFRO and JHN

In order to test the hypothesis that *FRO* gene may also play roles in iron homeostasis. Hydroponics experiment was conducted to compare MuFRO and JHN wild type at tillering stage in normal and toxic levels of Fe nutrient solution (Yoshida, 1976) for three weeks. As a result under control condition MuFRO maintained 136% higher iron shoot content than the wild type whereas the dry weights of both samples were not significantly different. While, under the Fe toxic condition MuFRO stayed greener and last longer than its wild type **(Figure 12)** but the shoot Fe content was 32% lower than JHN **(Table 4)**. It seems that Fe in shoot of MuFRO was lower than JHN. The fact that MuFRO grown better than JHN in the toxic condition, the lower shoot Fe content may simply reflect the dilution effect. This result may address the reason why JHN is not as tolerant as MuFRO when grown in Fe toxic nutrient solution.

Table 4 Iron contents on the stem and leave of JHN compare with MuFRO grown under control (4 ppm Fe) and Fe toxic (300 ppm Fe) nutrient solution

Name	control			toxic		
	stem	leave	Total in shoot	stem	leave	Total in shoot
JHN	9.57	17.72	27.29	476.17	371.68	847.85
MuFRO	35.52	28.92	64.44	204.18	435.51	639.69

Figure 12 Characterization of holistic phenotype of (a) wild-type and (b) MuFRO. A left site is the visible phenotype under toxic nutrient solutions (300 ppm FeEDTA) for three weeks. A right site is the phenotype under control (4 ppm Fe) condition

7. Development of gene-specific markers for MAS

Bi-directional SNP primers utilizing four primers in a single PCR amplification were developed. Primers were designed based on the guidelines proposed by Liu *et al.* (1997). Two sets of bi-directional SNP primers were developed for genotyping of SAP on exon 4 and exon 5 of the *OsFRO1* gene **(Table 5)**. Target DNA was amplified followed the KAPA 2G Robust HS protocol (KAPABIOSYSTEMS) under the following thermal cycling conditions: one cycle at 95 °C for 3 min, 35 cycle of a 30-s denaturation at 95 °C, a 30-s annealing at 61 °C and a 30-s extension at 72 °C and a final extension at 72 °C for 2 min. The PCR products were examined by electrophoresis on 1.2% agarose gel **(Figure 13)**.

Table 5 The list of bi-directional SNP primer sequence

Name	Sequence 5' → 3'
OsFRO1_Ex.4F	GGTGGATGAAGACACTACTGC
OsFRO1_Ex.4R	CACAGGACATTGGTCATAGCA
OsFRO1_Ex.4_SAP_A	GGCCTCCGGTTCGGATCGA
OsFRO1_Ex.4_SAP_G	GCCATGCAAAACAACCCGAC
OsFRO1_Ex.5F	TCATCTACTCTGTTTTGGAGGT
OsFRO1_Ex.5R	CTTGCTGGCTTTGAGAAGACT
OsFRO1_Ex.5_SAP_G	TTCCTGAGGTTCTGGCAATG
OsFRO1_Ex.5_SAP_C	TGTCCACCTTGGCCCTGG

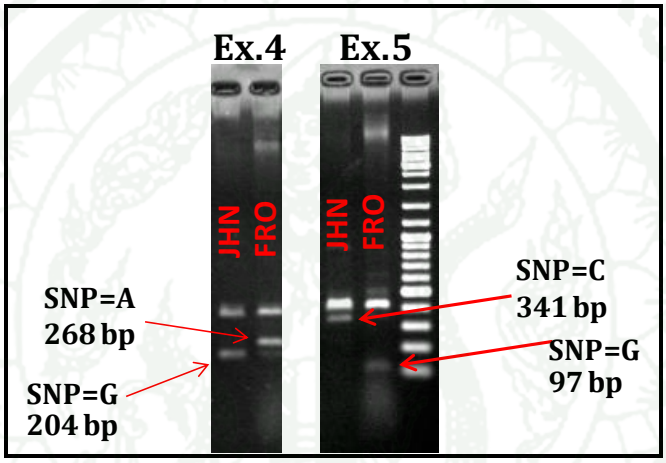

Figure 13 Genotyping JHN and MuFRO using the Bi-directional SNP primers for a Single Amino Acid Change (SAP) on exon 4 and 5**.** An expected amplicon size of SAP of exon 4 as SAPEx.4 F/R=435 bp, SAP_A/SAPEx.4_R=268 bp and SAPEx.4F/SAP-G=204 bp. While, expected amplicon size of SAP on exon 5 as SAPEx.5 F/R=402 bp, SAPEx.5F/SAP-C=341 bp and SAP_G/SAPEx.5_R=97 bp

Table 6 Genotyping on two SAPs position on *OsFRO1*, Indel on 5'UTR *OsFer1* and the Fe phenotype (Fe toxic in seedling and grain PPB score) on selected mutants with tolerant or susceptible to Fe toxicity and standard cultivars

FRO1	*OsFRO1* Exon.4	*OsFRO1* Exon.5	*OsFer1* 5'UTR	Fe toxic	PPB Score
1463	G/A	C/G	TATATACACA	Tolerant	+
3130	G/A	C/G	TATATACACA	Tolerant	+
11183	G/A	C/G	TATATACACA	Moderate	++
MuFRO	A	G	TATATACACA	Tolerant	++
Mu783	G/A	C/G	TATATACACA	Tolerant	+
8097	G	C	TATATACACA	Moderate	0
8419	G	C	TATATACACA	Moderate	0
2550	G	C	TATATACACA	Tolerant	+
2532	G	C	TATATACACA	Tolerant	+
3099	G	C	TATATACACA	Tolerant	+
3113	G	C	TATATACACA	Tolerant	+
2544	G	C	TATATACACA	Tolerant	+
2546	G	C	TATATACACA	Tolerant	+
2559	G	C	TATATACACA	Tolerant	+
4906	G	C	TATATACACA	Susceptible	++
2404	G	C	TATATACACA	Susceptible	+
2445	G	C	TATATACACA	Susceptible	+
2491	G	C	TATATACACA	Susceptible	+
2566	G	C	TATATACACA	Susceptible	+
2573	G	C	TATATACACA	Susceptible	+
2581	G	C	TATATACACA	Susceptible	+
3117	G	C	TATATACACA	Susceptible	+
3158	G	C	TATATACACA	Susceptible	+
3166	G	C	TATATACACA	Susceptible	+
3295	G	C	TATATACACA	Susceptible	+
MuMT1	G	C	TATATACACA	Susceptible	++
MuMT2	G	C	TATATACACA	Susceptible	++
JHN	G	C	TATATACACA	Moderate	+
KDML	A	G	-	Moderate	0
IR68144	G	C	TATATACACA	Susceptible	++
Pinkaset#3	A	G	-	Moderate	0
RIL (KD/JHN# 909-21-2-5)	A	G	-	Tolerant	0

Genotyping results of two SAPs position on *OsFRO1* and Indel on 5'UTR *OsFer1* in 27 selected mutants and 5 standard varieties with differing significantly on Fe toxicity tolerance phenotype. The results showed that 2 SAP on *OsFRO1* were found on 5 mutant lines as 1463, 3130, 11183, MuFRO, Mu783 and 3 natural varieties with Fe-toxic tolerant phenotype at seedling stage. While, there were not

found these SAPs on susceptible lines. However, several Fe-toxic tolerant mutant lines still have the same genotype on *OsFRO1* with JHN wild type. It seems that, Fe toxicity tolerance may influence by other genes. For the sequence variation on 5'UTR *OsFer1*, there were not detected polymorphism among these mutants. This result confirmed that the previous reverse screening by DHPLC.

Part III: Identification of candidate genes for grain Fe density

1. Mutant lines selection

Forward screening required high throughput phenotyping for isolation of mutants. There is a lack of efficient methods of mutant gene identification in forward screening by SFP. Two extremely mutants for grain iron were applied to survey genome-wide mutation. The highest grain Fe density mutant that contains 29 ppm Fe and the lowest mutant that contain only 7 ppm grain Fe **(Table 7**).

Table 7 Grain iron density of two extreme mutant lines and JHN wild type analyzed by three methods as PPB, AAS and ICP

Lines	PPB Score	AAS(mg/kg)	ICP(mg/kg)
Jao Hom Nin	+	12.93	12.3
4643	++	25.26	29.2
8097	0	8.83	7.3

2. Genome-wide mutation screening

In order to rapidly identify mutations by forward screening, SFP was applied following Kumar *et al.* (2007) to survey two extreme mutants for grain iron. Genome-wide screened for SFP was conducted using 57K Rice GeneChip expression array that was designed to hybridize with 57,000 genes-coding sequence (Dash *et al.*, 2012). Using 30% FDR, 32 and 45 SFPs were distinctive in Mu4643 (high Fe) and Mu8097 (low Fe), respectively from the wild type **(Appendix Table 3 and 4).**

Surprisingly, no known iron-related candidate genes were identified by SFP on high Fe (Mu4643). Specific SFPs which hybridized differential between high Fe (Mu4643) which is expressed proteins, hypothetical proteins and transposons. Interestingly, 4 SFPs-related genes on low Fe mutant Mu8097 had shown the putative function on Fe homeostasis.

3. SFP confirmation by direct sequencing

Nucleotide sequence alignment between JHN wild type and low Fe mutant (Mu8097) were identified newly SNPs **(Table 8)** in cation transporter candidate genes including *PDR-like ABC transporter* (LOC_Os11g37700), *Zinc finger* (LOC_Os11g36430), *Indole-3-glycerol phosphate lyase* (LOC_Os03g58260), and *Chlorophyll a oxygenase* or *Lethal leaf spot1* (LOC_Os03g59152). SAPs were identified on 3 genes as LOC_Os03g59152, LOC_Os11g36430 and LOC_Os11g37700. Whereas, on LOC_Os03g58260 can identify only SNPs on 3' UTR.

Table 8 SNPs and indel on SFP iron-related genes in low iron mutant (Mu8097)

Chr	Loc.	JHN	Mu4643	Mu8097	MuFRO	Nipponbare	Location of SNP
3	LOC_Os03g58260	C	C	T	C	C	3'UTR
3	LOC_Os03g59152	C	C	T	C	C	Exon 4 (T>I)
				CGCCGTCGTGGCTG			Inton4
3	LOC_Os03g59152	-	-	CGGCTGTGCTGTGC	-	-	
3	LOC_Os03g59152	C	C	A	C	C	Inton4
3	LOC_Os03g59152	AGACT	AGACT	-	AGACT	AGACT	Inton4
11	LOC_Os11g36430	-	-	AAT	-	-	Exon4 (->N)
11	LOC_Os11g36430	A	A	G	A	A	Exon 4
11	LOC_Os11g36430	T	T	C	T	T	Exon 4 (I>T)
11	LOC_Os11g36430	G	G	A	G	G	Exon 4 (A>T)
11	LOC_Os11g36430	T	T	C	T	T	Exon 4
11	LOC_Os11g36430	A	A	G	A	G	Exon 4
11	LOC_Os11g36430	T	T	A	T	T	Exon 4
11	LOC_Os11g36430	-	-	TG	-	-	3 UTR
11	LOC_Os11g36430	C	C	T	C	C	3'UTR
11	LOC_Os11g36430	A	A	T	A	A	3'UTR
11	LOC_Os11g36430	T	T	A	T	T	3'UTR
11	LOC_Os11g36430	A	A	G	A	A	3'UTR

Table 8 (Continued)

Chr	Loc.	JHN	Mu4643	Mu8097	MuFRO	Nipponbare	Location of SNP
11	LOC_Os11g37700	G	G	A	G	G	Exon 20
11	LOC_Os11g37700	T	T	C	T	T	Exon 20
11	LOC_Os11g37700	C	C	T	C	T	Exon 20
11	LOC_Os11g37700	G	G	A	G	G	Exon 20 (S>N)
11	LOC_Os11g37700	G	G	A	G	G	Exon 20 (V>I)
11	LOC_Os11g37700	A	A	G	A	A	Exon 20 (T>A)
11	LOC_Os11g37700	A	A	G	A	A	Exon 20 (I>V)
11	LOC_Os11g37700	G	G	A	G	G	3'UTR
11	LOC_Os11g37700	C	C	-	C	C	3'UTR
11	LOC_Os11g37700	G	G	C	G	G	3'UTR
11	LOC_Os11g37700	G	G	A	G	G	3'UTR

4. Expression analysis of SFP-related genes

RT-PCR from 14 days seedling was performed by using QIAGEN OneStep RT-PCR standard protocol (QIAGEN OneStep RT-PCR Kit Handbook, 2008). The results showed that the transcription level of *PDR, Zinc finger* and *Indole-3-glycerol phosphate lyase* was highly decreased in Mu8097. However, no differential expression in *Chlorophyll a oxygenase,* but the RT-PCR product size of low Fe (Mu8097) was larger than JHN.

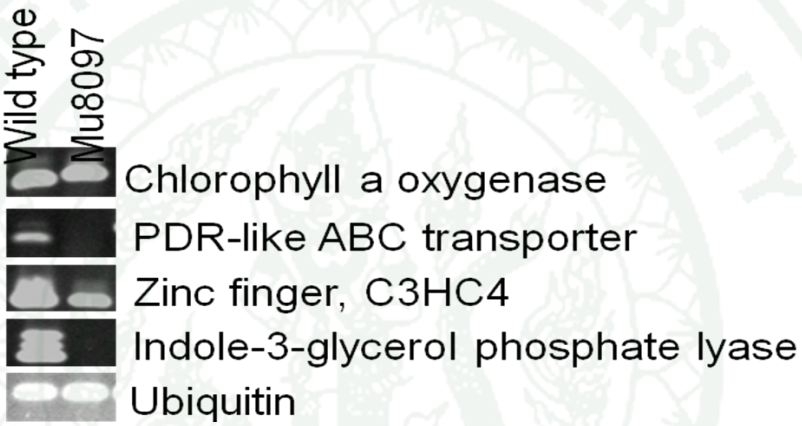

Figure 14 RT-PCR analyses of four iron-related gene mutants identified from SFP between JHN and low Fe mutant (Mu8097). Total RNA was isolated from shoot of 14 days old seedling

5. Genomic characterization of SFP-related genes

5.1 Genomic characterization of LOC_Os03g59152

LLS1 or *CaO* structure consists of pheophorbide a oxygenase (PaO) domain. This domain was found in bacterial and plant proteins to the C-terminus of a Rieske 2Fe-2S domain (pfam00355). Pheophorbide a oxygenase (PaO) which seems to be a key regulator of chlorophyll catabolism. Arabidopsis PaO (AtPaO) is a Rieske-type 2Fe-2S enzyme that is identical to Arabidopsis *accelerated cell death 1* and homologous to *lethal leaf spot 1 (LLS1)* of maize, in which the domain described here is also found.

The genomic region of LOC_Os03g59152: *lethal leaf spot1* (*LLS1*) in JHN and low Fe mutant (Mu8097) was sequenced and the major polymorphisms were identified **(Table 8)**. Two indels were found to be located in intron 4 (5 bp deletion and 28 bp insertion in 8097 alleles). Two SNPs were identified in 8097 including 1 nonsynonymous SNP in exon 4, and 1 SNP on intron 4. More significantly, the 28 bp insertion in intron 4 was affected an alternative splicing in Mu8097 **(Figure 14**). Furthermore, protein translation by using ExPASy translate tool result of Mu8097 by merging 28 bp insertion and a surround sequence in Mu8097 found that major variation on C-terminus. The number of amino acids in 8097 was higher 9 amino acids than JHN that make 262 total amino acid. Moreover, from the terminal amino acids at the 223th position to the stop codon on Mu8097, amino acid sequence was different from its wild type. This RT-PCR result was also confirmed this alternative splicing in booting panicle and flag leaf at flowering stage of Mu8097 **(Figure 15**).

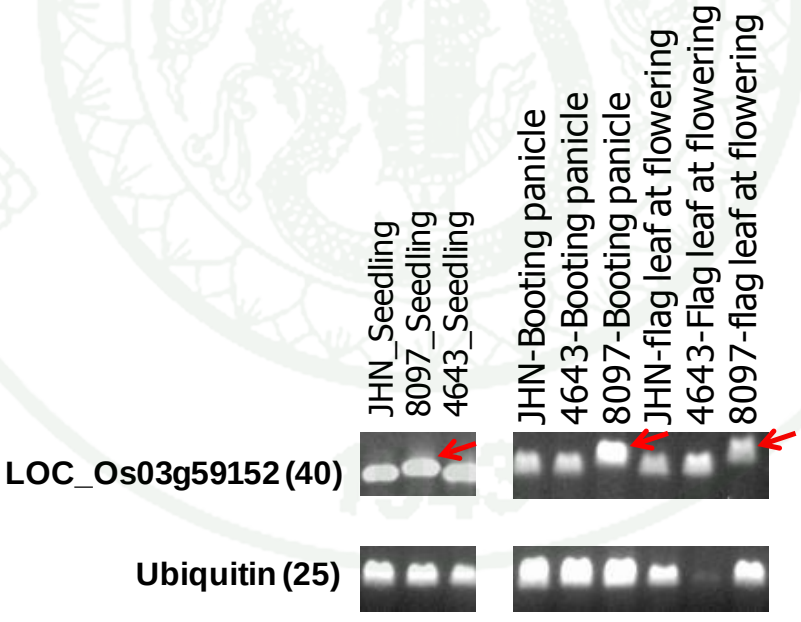

Figure 15 RT-PCR analysis of LOC_Os03g59152 between JHN, high (Mu4643) and low Fe mutant (Mu8097). Total RNA was isolated from shoot of 14 days old seedling, booting panicle and flag leaf at flowering stage

```
Nip       MKMRIEEASIDGFHSNLDGDWGYFKFVAPCTLYGTPFRTDLEADEVKKKKKKKPEVRVVL 60
JHN       MKMRIEEASIDGFHSNLDGDWGYFKFVAPCTLYGTPFRTDLEADEVKKKKKKKPEVRVVL 60
8097      MKMRIEEASIDGFHSNLDGDWGYFKFVAPCTLYGTPFRTDLEADEVKKKKKKKPEVRVVL 60
          ************************************************************

Nip       FTVPVAPGRSRFIWASRYKVGGWLDKILPRWFYHMTSNTILDSDTYLHVEDRNITTVGLD 120
JHN       FTVPVAPGRSRFIWASRYKVGGWLDKILPRWFYHMTSNTILDSDTYLHVEDRNITTVGLD 120
8097      FTVPVAPGRSRFIWASRYKVGGWLDKILPRWFYHMTSNTILDSDTYLHVEDRNITTVGLD 120
          ************************************************************

Nip       NWHKACYVPTSSDNLVIAYRNWFRKYCNHQIGWANPNPTVKQQLPQTPTRDQLLERYWSH 180
JHN       NWHKACYVPTSSDNLVIAYRNWFRKYCNHQIGWANPNPTVKQQLPQTPTRDQLLERYWSH 180
8097      NWHKACYVPTSSDNLVIAYRNWFRKYCNHQIGWANPNPTVKQQLPQTPTRDQLLERYWSH 180
          ************************************************************

Nip       VMQCTSCRAALKGMRALEITLQVAAVAVVGFLAAGKETAVMSEAR------PGIQSFSLS 234
JHN       VMQCTSCRAALKGMRALEITLQVAAVAVVGFLAAGKETAVMSEAR------PGIQSFSLS 234
8097      VMQCTSCRAALKGMRALEIILQVAAVAVVGFLAAGKETAVMSGVQRAAVVAAAVLCFAAS 240
          ****************** ********************** .:      ..: .*: *

Nip       KNKRSQATAKGIHEETASA-- 253
JHN       KNKRSQATAKGIHEETASA-- 253
8097      RWLANFIEKTFYFQDYVHADK 261
          :   .    .  .:: . *
```

Figure 16 Amino acid sequence alignment on LOC_Os03g59152 of JHN, Mu8097 and ref. Nipponbare. The 223th position of the stop codon on Mu8097, amino acid sequence was different from its wild type is highlighted in gray

The 223th position until the stop codon on Mu8097 was differed from JHN The sequence "GVQRAAVVAAAVLCFAASRWLANFIEKTFYFQDYVHADK" were searched by Blast P on NCBI. The result showed that the amino acid sequence was 100% identities with hypothetical protein (OsI_13979) on the indica rice genome. Moreover, Full-length amino acid sequence of the OsI_13979 and translated sequence of Mu8097 were 99 % sequence identities. Both of proteins also contain the Pheophorbide a oxygenase (pfam08417) domain similar than the *LLS1*.

```
Hypo OsI_13979    MKMRIEEASIDGFHSNLDGDWGYFKFVAPCTLYGTPFRTDLEADEVKKKKKK-PEVRVVL 59
Protein_8097      MKMRIEEASIDGFHSNLDGDWGYFKFVAPCTLYGTPFRTDLEADEVKKKKKKKPEVRVVL 60
                  ************************************************* *******

Hypo OsI_13979    FTVPVAPGRSRFIWASRYKVGGWLDKILPRWFSHMTSNTILDSDTYLHVEDRNITTVGLD 119
Protein_8097      FTVPVAPGRSRFIWASRYKVGGWLDKILPRWFYHMTSNTILDSDTYLHVEDRNITTVGLD 120
                  ******************************** ************************

Hypo OsI_13979    NWHKACYVPTSSDNLVIAYRNWFRKYCNHQIGWANPNPTVKQQLTQTPTRDQLLERYWSH 179
Protein_8097      NWHKACYVPTSSDNLVIAYRNWFRKYCNHQIGWANPNPTVKQQLPQTPTRDQLLERYWSH 180
                  ******************************************.***************

Hypo OsI_13979    VMQCTSCRAALKGMRALEIILQVAAVAVVGFLAAGKETAVMSGVQRAAVVAAAVLCFAAS 239
Protein_8097      VMQCTSCRAALKGMRALEIILQVAAVAVVGFLAAGKETAVMSGVQRAAVVAAAVLCFAAS 240
                  ************************************************************

Hypo OsI_13979    RWLANFIEKTFYFQDYVHADK 260
Protein_8097      RWLANFIEKTFYFQDYVHADK 261
                  *********************
```

Figure 17 Amino acid sequence alignment of the hypothetical protein OsI_13979 and translated sequence of Mu8097. The underlines were the Pheophorbide a oxygenase (pfam08417) domain

Furthermore, the stretch of amino acid sequence on Mu8097 was similar to nearby gene LOC_Os03g59110, an oxidoreductase in japonica rice genome. So the insert size may be inframed with and expand from 28 bp to the stop codon **(Figure 18)**.

The 28 bp insertion was developed for indel marker. Specific primers to the following genes were used: F 5'_ATGTCATGCAGTGCACCAGT_3' and R 5'_AGCCCAGGTTCATGACAAAT_3'. An expected amplicon size of indels was 282 bp (JHN) or 310 bp (Mu8097). This marker was screened on 23 reference standard cultivars and iron mutants set. The results showed that the 28 bp insertion was found in standard cultivars as IR68144 and Pinkaset#2 allele. Moreover, there were 3 new iron mutants were carried the 28 bp insertion **(Appendix table 5)**.

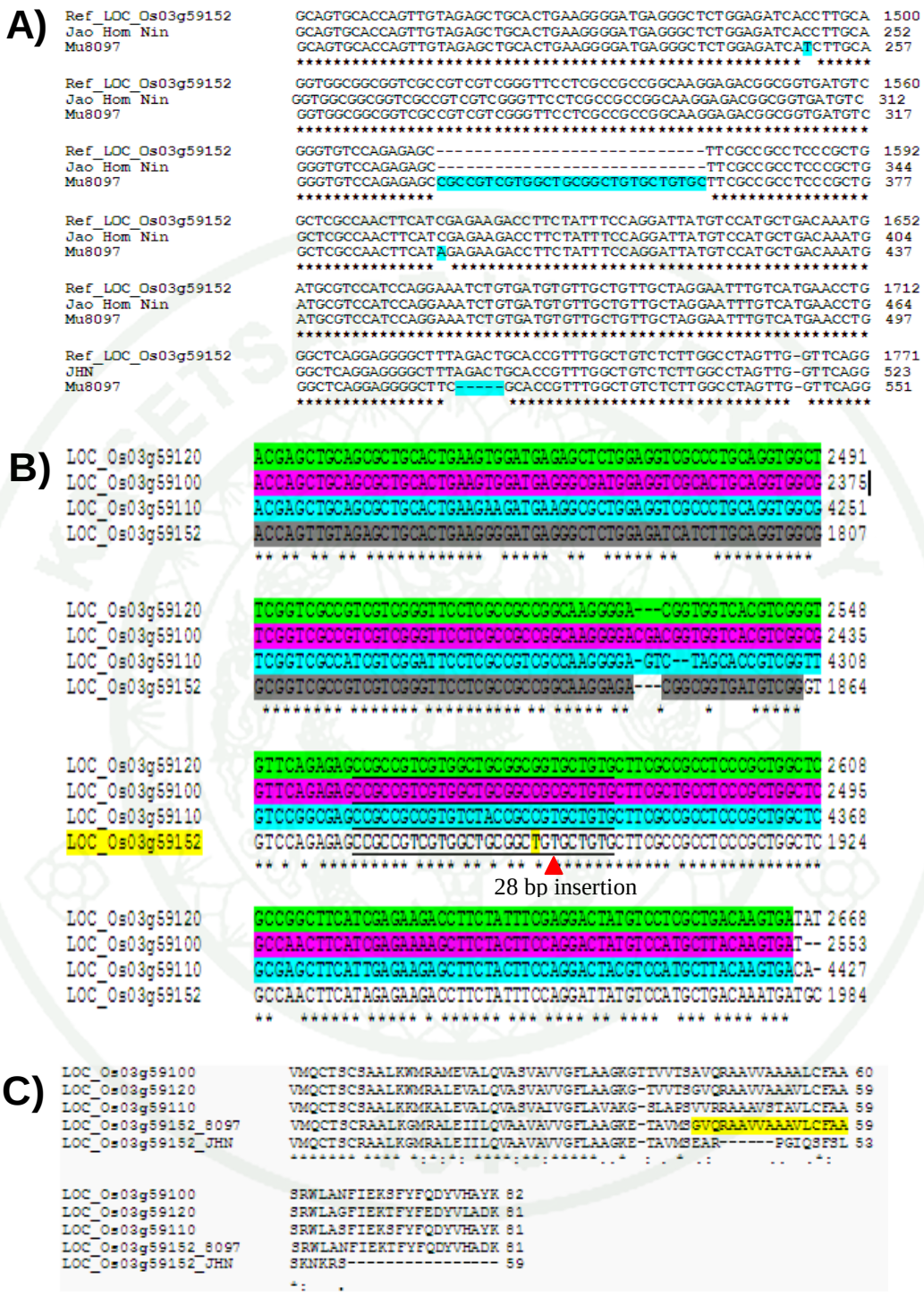

Figure 18 A) Multiple sequence alignment of *LLS1* compare between JHN, Mu8097 and ref. sequence from Nipponbare. B) The 28 bp insertion and ~200 bp flanking sequence identical to a conserved motif found in three nearby oxidoreductase genes on chromosome 3. C) Amino acid sequence alignment between 4 homolog *LLS1*

5.2 Genomic characterization of LOC_Os11g36430

The genomic region of LOC_Os11g36430*: Zinc finger*, C_3HC_4 type domain containing protein in JHN and low Fe mutant (Mu8097) was sequenced and compared and major polymorphisms were identified **(Table 8)**. One 2 bp-insertion was found to be located in the 3'UTR. In the coding sequence, an in-frame 3-bp insertion was present in exon 4 of 8097. Ten SNPs was identified in 8097 including 2 nonsynonymous SNPs, 4 synonymous SNPs in exon 4 and 4 SNPs on 3' UTR. More significantly, 1 nonsynonymous SNP in exon 4 with was predicted effect of the loss of function on USP7 NTD domain (Pattern = [PA][^P][^FYWIL]S[^P]) in 8097.

Zinc finger (Znf) domains are relatively small protein motifs which contain multiple finger-like protrusions that make tandem contacts with their target molecule. Some of these domains bind zinc, but many do not; instead binding other metals such as iron or no metal at all (http://www.ebi.ac.uk/interpro/entry /IPR018957). Based on the presence of this important SAP in 8097, LOC_Os11g36430 mRNA may be subjected to post-transcriptional degradation, and the absence of this mRNA may responsible for the low grain iron storage observed in Mu8097.

```
JHN             MASGTDEKAKMEGLTSAAAFVEGGIQDACDDACSICLEAFCESDPSTLTGCKHEFHLQCI
8097            MASGTDEKAKMEGLTSAAAFVEGGIQDACDDACSICLEAFCESDPSTLTGCKHEFHLQCI
                ************************************************************

JHN             LEWCQRSSQCPMCWQPISLKDPTSQELLEAVERERNVRTNQTRNTTIFHHPALGDFEVQH
8097            LEWCQRSSQCPMCWQPISLKDPTSQELLEAVERERNVRTNQTRNTTIFHHPALGDFEVQH
                ************************************************************

JHN             LPVVGNDAELEERILQHLAAAAAMGRSHHLGRREGHRGRSGSHGRPQFLVFSSHPNMPSA
8097            LPVVGNDAELEERILQHLAAAAAMGRSHHLGRREGHRGRSGSHGRPQFLVFSSHPNMPSA
                ************************************************************

JHN             GSVSSSSVQGEVDNESSPVHTTGELSLHANTHEEAGNQSPGMLTYDADQDAVVSSGNSTP
8097            GSVSSSSVQGEVDNESSPVHTTGELSLHANTHEEAGNQSPGMLTYDADQDAVVSSGNSTP
                ************************************************************

JHN             VSSPRFFNRRHSTGQSTPVNNDRAGPSDLQSFSDSLKSRLNAVSMKYKESITKSTRGWKE
8097            VSSPRFFNRRHSTGQSTPVNNDRAGPSDLQSFSDSLKSRLNAVSMKYKESITKSTRGWKE
                ************************************************************

JHN             RLFSRHSSVADLGSEVRREVNAGIASVSRMMERLETRGSN-GRTSDGPAISTSEVIPSTE
8097            RLFSRHSSVADLGSEVRREVNAGIASVSRMMERLETRGSNNGRTSDGPATSTSEVIPSTE
                ************************************* ******** **********

JHN             SSNERVTENNPTTAATSSGNTSASSAPCVTTTDSN
8097            SSNERVTENNPTTAATSSGNTSTSSAPCVTTTGSN
                **********************:*********.**
```

Figure 19 Amino acid sequence alignment of the JHN and Mu8097 alleles of LOC_Os11g36430. The conserved USP7 NTD domain is underlined, and the SAP in the 8097 alleles is highlighted in gray

5.3 Genomic characterization of LOC_Os11g37700

The genomic region of LOC_Os11g37700*:* pleiotropic drug resistance protein, putative (*OsPDR3*) in JHN and low Fe mutant (Mu8097) was sequenced and the major polymorphisms were identified **(Table 8)**. Eleven SNPs were identified in 8097 including 4 nonsynonymous SNPs, 3 synonymous SNPs in exon 20 and 4 SNPs on 3' UTR.

Pleiotropic drug resistance protein (*OsPDR*) is a member of plant ABC transporters. Fourmeau (2010) reported that *AtPDR9* expression was found to be induced by iron deficiency and both proteins appeared to localize to the plasma membrane of the root epidermal cells. The characterization of Arabidopsis mutant plants that do not express *AtPDR9* revealed that the mutant plants were less tolerant to iron-deficient conditions than wild type plants, displaying a stronger chlorosis and growth retardation when not supplied with iron. On this experiment, *OsPDR3*

(LOC_Os11g37700) was suppressed expression in low Fe mutant line (Mu8097) at 14 days seedling stage.

```
JHN             RTVFYRERAAGMYSSLSYAFAQACVEVIYNILQGILYTIIIYAMIGYDWKADKFFYFMFF 1320
MU8097          RTVFYRERAAGMYSSLSYAFAQACVEVIYNILQGILYTIIIYAMIGYDWKADKFFYFMFF 1319
                ************************************************************

JHN             IVASFNYFTLFGMMLVACTPSAMLANILISFVLPLWNLFAGFLVVRPLIPIWWRWYYWAN 1380
MU8097          IVASFNYFTLFGMMLVACTPSAMLANILISFVLPLWNLFAGFLVVRPLIPIWWRWYYWAN 1379
                ************************************************************

JHN             PVSWTIYGVVASQFGKNGDVLSVPGGSPTVVKQFLEDNLGMRHSFLGYVVLTHFGYIIVF 1440
MU8097          PVSWTIYGVVASQFGKNGDVLSVPGGSPTVVKQFLEDNLGMRHNFLGYIVLAHFGYVIVF 1439
                ****************************************.****:**:****:***

JHN             FFIFGYAIKYFNFQKR 1456
MU8097          FFIFGYAIKYFNFQKR 1455
                ****************
```

Figure 20 Amino acid sequence alignment of the JHN and Mu8097 alleles of *OsPDR3*. The single amino acid change is highlighted in gray

Discussion

Part I: Potential of using natural variation for grain Fe density and bioavailability

To meet the ultimate goal of 50 mg/kg is challenging. In this study, the most successful donor of high Fe density has been varieties of purple rice such as local landrace and wild rice (*O.nivara*), Several advance lines derived from a cross between *Oryza nivara*, a wild progenitor of cultivated rice and JHN, the intermediate iron dense rice. However, the highest Fe variety from *O.nivara*/JHN were low in Fe bioavailability and need to improve further. Furthermore, grain iron density among these varieties were variable on planting season (Vanavichit *et al*, 2008).

The major limitations to the use these purple rice germplasm are high phytic acid and tannin contents of the brown rice. Although phytic acid and tannin are considered antioxidants, they inhibit Fe bioavailability. Because white color rice is in general low in phytic acid and tannin, attempts were made to transmit high iron density from purple to white rice. Nonetheless, not all white rice varieties has high Fe bioavailability, Rigorous search for effective donors found two local landraces HPM (white) and KDC (black) generated progenies with promising Fe density and bioavailability. In a Fe bioavailability analysis on selected progenies from this population, we found that total phytate (Inositol pentaphosphate: IP5 + Inositol Hexaphosphate: IP6) significantly affected Fe bioavailability. High phytic acid (IP5+IP6) content was associated with low Fe bioavailability lines from HPM/KDC population. This result was in agreement with Hemalatha *et al* (2007). Furthermore, the effect of phytate on Fe bioavailability was also reported in Sorghum (Elkhalil, *et al* 2001). Moreover, Afify *et al* (2011) demonstrated the strategy to reduce phytate content and increase iron and zinc *in vitro* bioavailability in sorghum by soaking or seed germination. However, reported by Glahn *et al* (2002) shown that phytic acid levels were not correlated with Fe bioavailability. Rice genotypes with low Fe bioavailability were noticeably darker to purple in color. Glahn *et al* (2002)

demonstrated that unknown compounds related to rice grain color may be a major factor limiting Fe bioavailability from unpolished rice.

High iron content rice with high bioavailability is highly valuable for human health. Previous efficacy study of iron-dense rice 'Sinlex' consumption on iron status in 108 boys with iron depletion at Wat Don Jun, Chiangmai, in 2008 showed that for 8 months, 91% of students who consumed iron-dense rice had hemoglobin increased. Compared to the control group, only 71% of the students showed increased hemoglobin (Prapaisri *et al.*, 2008). New cross –breeding lines not only contain high grain Fe density but also high Fe bioavailbility in brown rice will be used for the iron biofortification program.

Rice breeding for tolerance to Fe toxicity to increase the rice production of iron in iron poisoning soil by using natural variation was limited by the variation in Fe toxic avoidance. The successful from a natural cross-hybridization selection can identify two Fe toxic tolerant RILs from KDML105/JHN cross, but the concentration of grain Fe is not higher than high Fe varieties planted in normal soil. The tolerance mechanism of RILs to be relevant to the rice plant in coping with excess iron concentrations with the oxidation power of the root (Ando, 1983) or exclusion of Fe in the rhizophere (Tadano, 1976). Thus, more excess iron cannot transport to whole plant and grain.

Part II: Identification of mutant lines conferring high grain Fe density and tolerance to Fe toxicity

Phenotypic distribution of grain Fe density and Fe toxicity tolerance among 12,000 base mutant lines were found that the highest and the lowest Fe density differs from natural variation. Furthermore, on Fe toxic screening, **(Figure 10)** high Fe dense mutants that can accumulation iron in rice seeds well in normal soil conditions and moderate resistant to iron toxicity and mutant lines contain moderate Fe content and Fe toxicity tolerance have a potential of the Fe toxicity area to improve grain iron

storage in rice. Induced mutation can produce both of a similar phenotype from natural variability and new extremely phenotypes.

Although forward screening can identify abundant Fe mutants, but the limitation is how to identify functional genes responsible for mutant phenotype. The first essential step is to trace for mutations on candidate gene sequences for effective marker development. In this study, we used dHPLC to screen for possible exon mutations on six candidate genes related to Fe uptake and transport. Only *OsFRO1* (LOC_Os04g36720) were identified. *OsFRO1* play role in the iron homeostasis. Two non-synonymous SNP on *OsFRO1* were found on Fe toxic tolerant phenotype both of mutant lines and natural cultivars at seedling stage. Well, there were not found these SNPs on susceptible lines. However, several Fe toxic tolerant mutant lines still have the same genotype on *OsFRO1* with JHN wild type. It seems that, Fe toxicity tolerances may be under control by other genes.

FN radiation can generate Fe mutants that can storage more grain Fe and/or tolerant to Fe toxic differ from natural variation. However, sequence variation in candidate genes of various mutant lines, sometime there were no different from sequence variations on public databases such as OryzaSNPs (http://oryzasnp.plantbiology.msu.edu). It seems that, induced mutations may accelerate the evolution of the genome faster than natural variation.

Part III: Identification of candidate genes for grain Fe density

FN radiation can generate new SNPs on new Fe-related genes. Newly SNPs were identified in several candidate genes including cation transporters such as PDR-like ABC transporter, Zinc finger, Indole-3-glycerol phosphate lyase, and Chlorophyll a oxygenase on the low Fe (Mu8097) by using SFP. Such gene may play important roles in Fe uptake from soil or Fe transportation to grains. However, whole-genome mutant screening by SFP on high Fe mutant (Mu4643) cannot identify mutations on known iron-related candidate genes. Specific SFPs which hybridized differential

between high Fe (Mu4643) were expressed proteins, hypothetical proteins and transposons. The rice genome array, designed for gene expression analyses, and contains probes to query 49,824 transcripts. Each probe set is represented by 11 probes/features and each probe is 25 bp long. The array contains only ~630,000 PM probes/features from rice (Kumar, *et al* 2007). Several mutations in rice genome out of the probe/features sequence cannot identify by SFP. However, the results of whole genome re-sequencing by using MiSeq from Illumina in Mu4643 were identified only 6 SNPs on 5 iron-related genes (from 44 selected Fe-related genes) when compare with JHN (Ruanjaichon *et al*., 2013). The 6 SNPs on Mu4643 were located in different regions of SFP probes/features. High grain iron density phenotype in Mu4643 may affect by another group of genes which no recently report function on Fe homeostasis.

The direct use of SFPs as "molecular markers" have been demonstrated in mapping genes associated with either qualitative (Borevitz *et al.,* 2003) or quantitative traits (Werner *et al.,* 2005; Wolyn *et al.,* 2004 and Hazen *et al.,* 2005) in Arabidopsis. In such QTL studies the probes generated from pooled DNA of RILs showing extreme of phenotypes were used for hybridization and prediction of SFPs. Based on allelic frequency differences in both extreme pools, QTLs containing candidate genes were mapped with high resolution by extreme array mapping (XAM) in the above studies. Detection of genomic changes using genome-wide chip on mutant rice was reported by Wu et al. (2005). On the mutant screening under similar genetic background, SFP was applied for screening between extreme mutants and wild type. However, SFP probes were designed based on unique sequence located on 3' UTR of genes. It seems that, a mutation on other regions cannot be identified by SFP.

CONCLUSION

Improvement of high grain iron density and bioavailability can be done using donors of natural genetic variation and mutagenesis. However, natural variation had main limitation on genetic variation for Fe uptake under Fe toxic condition. Alternatively, mutation breeding based-on TILLING, can generate wide variation on both content and uptake of Fe under even low pH soil conditions. Two extreme mutants were selected having highest and lowest grain Fe density, contained 29 ppm (Mu4643) and 7 ppm (Mu8097), respectively. Under Fe toxic screening, we found that mutants for tolerance to moderately tolerance to Fe toxicity level could as well accumulate more seed iron well in normal soil conditions.

On reverse genetic screening, two SAPs on *OsFRO1* were identified. This mutation related to Fe toxicity tolerance phenotype at seedling stage. Furthermore, whole-genome mutation screening by SFP was utilized to survey two extreme mutants, Mu4643 and Mu8097, for grain iron. Using 30% FDR, 32 and 45 SFPs were distinctive in JHN 4643 (high Fe) and 8097 (low Fe), respectively from the wild type. Newly mutations on new 4 iron transporter genes were identified on low Fe mutant. Interesting mutant with 28 bp insertion on *LLS1* (LOC_Os03g59152) in low Fe mutant affects an alternative splicing result in C-terminal amino acid change. However, no known iron homeostasis gene was identified on high Fe mutant.

That fact that mutagenesis by fast neutron induced rare genetic variation that may be lost in nature, TILLING can be viewed as important secondary gene pool for modern plant breeding program.

LITERATURE CITED

Afify, A.E.-M.M.R., H.E.S. El-Beltagi, S.M. Abd El-Salam, A.A. Omran. 2011. Bioavailability of iron, zinc, phytate and phytase activity during soaking ar germination of white sorghum varieties. **PLoS ONE.** 6(10): e25512.

Alexander, A. T. J., B. Kyriacou, D. L. Callahan, L. Carruthers, J. Stangoulis, E. Lombi, M. Tester. 2011. Constitutive overexpression of the *OsNAS* gene family reveals single-gene strategies for effective iron- and zinc-biofortification of rice endosperm. **PLOS ONE.** 6: e24476.

Alonso, J. M. and J. R. Ecker. 2006. Moving forward in reverse: genetic technologies to enable genome-wide phenomic screens in Arabidopsis. **Nat Rev Genet**. 7: 524–536.

_____, _____, A. N. Stepanova, T. J. Leisse, C. J. Kim, H. Chen, P. Shinn, D. K. Stevenson, J. Zimmerman, P. Barajas, R. Cheuk, C. Gadrinab, C. Heller, A. Jeske, E. Koesema, C. C. Meyers, H. Parker, L. Prednis, Y. Ansari, N. Choy, H. Deen, M. Geralt, N. Hazari, E. Hom, M. Karnes, C. Mulholland, R. Ndubaku, I. Schmidt, P. Guzman, L. Aguilar-Henonin, M. Schmid, D. Weigel, D.E. Carter, T. Marchand, E. Risseeuw, D. Brogden, A. Zeko, W.L. Crosby and C.C. Berry. 2003. Genome-wide insertional mutagenesis of Arabidopsis thaliana. **Science**. 301: 653–657

Ando, T. 1983. Nature of oxidizing power of rice roots. **Plant and Soil**. 72:57-71

AOAC. 2000. **Official method of analysis of the association of official analytical chemists.** 17th ed. Method. Association of official analytical chemists, Gaitherburg, MD., USA.

Arbelt, W. 2003. **Developing a Standardized Procedure to Screen Lowland Rice (*Oryza sativa*) Seedlings for Tolerance to Iron Toxicity.** M.Sc. Thesis, Rheinischem Friedrich-Wilhelms University.

Asch, F., M. Backer and D.S. Kpongor. 2005. A Quick and efficient screen for tolerance to iron toxicity in lowland rice. **J. Plant Nutri. and Soil Sci.** 168: 764-773.

Audebert, A. and K. L. Sahrawat. 2000. Mechanisms for iron toxicity tolerance in lowland rice. **Plant Nutrition.** 23(11-12): 1877-1885.

Baker, J. R. 1958. **Principles of biological microtechnique,** pp 304. A study of fixation and dyeing. London.

Belouchi, A., T. Kwan and P. Gros. 1997. Cloning and characterization of the OsNramp family from *Oryza sativa*, a new family of membrane proteins possibly implicated in the transport of metal ions. **Plant Mol Biol**. 33: 1085-1092.

Bolle, C., A. Schneider and D. Leister. 2011. Perspectives on systematic analyses of gene function in Arabidopsis thaliana: new tools, topics and trends. **Curr Genomics**. 12(1): 1–14

Borevitz, J. O., D. Liang, D. Plouffe, H. S. Chang, T. Zhu, D. Weigel, C. C. Berry, E. Winzeler and J. Chory. 2003. Large-scale identification of single-feature polymorphisms in complex genomes. **Genome Res**. 13: 513–523.

Branda, S. S., Z. Yang, A. Chew and G. Isaya. 1999. Mitochondrial intermediate peptidase and the yeast frataxin homolog together maintain mitochondrial iron homeostasis in Saccharomyces cerevisiae. **Hum. Molec. Genet.** 8: 1099-1110.

Briat, J-F. and S. Lobreaux. 1997. Iron transport and storage in plants. **Trends in Plant Sci.** 2: 187-193.

Brune, M., I. Hallbergs and A.B. Skanberng. 1991. Determination of iron binding phenolic groups in foods. **J Food Sci.** 56: 128-131.

Caulder, D. L. and K. N. Raymond. 1998. The rational design of high symmetry coordination clusters. **J. Chem. Soc. Dalton Trans.** 1185-1200.

Chen, C. C., J. B. Dixon and F. T. Turner. 1980a. Iron coatings on rice roots: Morphology and models of development. **Soil Sci. Soc. Am. J.** 44, 1113–1119.

_____, _____, _____. 1980b. Iron coatings on rice roots: Mineralogy and quantity influencing factors. **Soil Sci. Soc. Am. J.** 44: 635–639.

Cheryan, M. 1980. Phytic acid interactions in food systems. **Crit. Rev. Food Sci. Nutr.** 13: 297-335.

Chew, A., G. Sirugo, J. P. Alsobrook and G. Isaya. 2000. Functional and genomic analysis of the human mitochondrial intermediate peptidase, a putative protein partner of frataxin. **Genomics.** 65: 104-112.

Crichton, R. R. and M. C. Wauters. 1987. Iron transport and storage. **Eur. J. Biochem.** 164: 485-506.

Curie, C., J. M. Alonso, M. Le Jean, J. R. Ecker and J. F. Briat. 2000. Involvement of NRAMP1 from *Arabidopsis thaliana* in iron transport. **Biochem J**. 347: 749-755.

_____, _____, Z. Panaviene, C. Loulergue, S. L. Dellaportaand E. L. Walker. 2001. Maize *yellow stripe*1 encodes a membrane protein directly involved in Fe (III) uptake. **Nature.** 409: 346-349.

Eckhardt, U., A. M. Marques and T. J. Buckhout. 2001. Two iron-regulated cation transporters from tomato complement metal uptake-deficient yeast mutants. **Plant Mol. Bio.** 45: 437–448.

Eide, D. J. 1998. The molecular biology of metal ion transport in *Saccharomyces cerevisiae*. **Annu. Rev. Nutr.** 18: 441-469.

Eide, D., M. Broderius, J. Fett and M. L. Guerinot. 1996. A novel iron-regulated metal transporter from plants identified by functional expression in yeast, pp. 5624–5628. *In* **Proceedings of the National Academy of Sciences**. USA.

Einset, J., P. Winge, A. M. Bones and E. L. Connolly. 2008. The FRO2 ferric reductase is required for glycine betaine's effect on chilling tolerance in Arabidopsis roots. **Physiol Plant**. 134(2): 334-41.

Elkhalil, EAI, A.H. El-Tinay, B.E. Mohamed and E.A.E. Elsheikh. 2001. Effect of malt pretreatment on phytic acid and *in vitro* protein digestibility of sorghum flour. **Food Chem** 72: 29–32.

Gibson, T. J., E. V. Koonin, G. Musco, A. Pastore and P. Bork. 1996. Friedreich's ataxia protein: phylogenetic evidence for mitochondrial dysfunction. **Trends Neurosci.** 19: 465-468.

Glahn, R. P., O. A. Lee, A. Yeung, M. I. Goldman and D. D. Miller. 1998. Caco-2 cell ferritin formation predicts nonradiolabeled food iron availability in an in vitro digestion/Caco-2 cell culture model. **Amer. Soc. Nutr. Sci.** 1555-1561.

Goto, F., T. Yoshihara, N. Shigemoto, S. Toki and F. Takaiwa. 1999. Iron fortification of rice seed by the soybean ferritin gene. **Nat. Biotechnol.** 17: 282–286.

Greene, E. A., C. A. Codomo, N. E. Taylor, J. G. Henikoff, B. J. Till, S. H. Reynolds, L. C. Enns, C. Burtner, J. E. Johnson, A. R. Odden, L. Comai and S. Henikoff. 2003. Spectrum of chemically inducedmutations from a large-scale reverse-genetic screen in Arabdiopsis. **Genetics**. 164: 731–740.

Gross, J., R. J. Stein, A. Germano, F. Neto and J. P. Fett. 2003. Iron homeostasis related genes in rice. **Gen. and Mol. Bio**. 26 (4): 477-497.

Guerinot, M. L. 2000. The ZIP family of metal transporters. **Biochimica et Biophysica Acta.** 1465: 190–198.

_____ and Y. Yi. 1994. Iron: nutritious, noxious, and not readily available. **Plant Physiol.** 104: 815–820.

Hallberg, L., M. Brune and L. Rossander. 1989. The role of vitamin C in iron absorption. Int. **J. Vitam. Nutr. Res. Suppl.** 30: 103-108.

Haas, E.M. n.d. Mineral: Iron. **Health World Online.** Available Source: http://www.healthy.net/scr/Article.asp?Id=2075, April 25, 2004.

Hazen, S. P., J. O. Borevitz, F. G. Harmon, J. L. Pruneda-Paz, T. F. Schultz, M. J. Yanovsky, S. J. Lilegren, J. R. Ecker, and S. A. Kay. 2005. Rapid array mapping of circadian clock and developmental mutations in Arabidopsis. **Plant Physiol**. 138: 990–997.

Hemalatha, S., K. Platel and K. Srinivasan. 2007. Zinc and iron contents and their bioaccessibility in cereals and pulses consumed in India. **Food Chem.** 102; 1328-1336.

Herbik, A. 1997. **Proteinchemische und molekularbiologische Charakterisierung der Tomatenmutante chloronerva.** PhD Thesis, Humboldt University, Berlin, Germany.

_____, A. Giritch, C. Horstmann, R. Becker, H. J. Balzer, H. Bäumlein and U.W. Stephan. 1996. Iron and copper nutrition-dependent changes in protein expression in a tomato wild type and the nicotianamine-free mutant *chloronerva*. **Plant Physiol.** 111: 533–540.

Higuchi, K., N. K. Nishizawa, H. Yamaguchi, V. Römheld, H. Marschner and S. Mori. 1995. Response of nicotianamine synthase activity to Fe-deficiency in tobacco plants as compared with barley. **J. Exp. Bot.** 289: 1061–1063.

Hirochika, H. 2010. Insertional mutagenesis with Tos17 for functional analysis of rice genes. **Breeding Sci**. 60: 486–492.

Hirschi, K. D. 2003. Strike while the ionome is hot: making the most of plant genomic advances. **TRENDS in Biotech**. 21 (12): 520-521.

Hurrell, R. F., M. A. Jullierat, M. B. Reddy, S. R. Lynch, S. A. Dassenko and J. D. Cook. 1992. Soy protein, phytate and iron absorption in humans. **Am. J. Clin. Nutr.** 56: 573-578.

Isaya, G. 2004. Future Directions & Projects. **Mayo Clinic Collage of Medicine**. Available Source: http://mayoresearch.mayo.edu/mayo/research/isayalab/futureprojects.cfm, August 15, 2004.

Illumina, 2013. **An Introduction to Illumina Next-Generation Sequencing Technology for Agriculture.**
Available Source: res.illumina.com/documents/.../app_spotlight_ngs_ag.pdf

Ishimaru, Y., M. Suzuki, T. Tsukamoto, K. Suzuki, M. Nakazono, T. Kobayashi, Y. Wada, S. Watanabe, S. Matsuhashi, M. Takahashi, H. Nakanishi, S. Mori and N. K. Nishizawa. 2006. Rice plants take up iron as an Fe^{3+}-phytosiderophore and as Fe^{2+}. **Plant J.** 45: 335–346.

_____, _____, _____, _____, _____, H. Masuda, K. Bashir, H. Inoue, H. Aoki, T. Hirose and R. Ohsugi. 2010. Rice metal-nicotianamine transporter, OsYSL2 is required for the long-distance transport of iron and manganese. **Plant J**. 62: 379–390.

Kawahara, Y., M. de la Bastide, J. P. Hamilton, H. Kanamori, W. R. McCombie, S. Ouyang, D. C. Schwartz, T. Tanaka, J. Wu, S. Zhou, K. L. Childs, R. M. Davidson, H. Lin , L. Quesada-Ocampo, B. Vaillancourt, H. Sakai, S. S. Lee, J. Kim, H. Numa, T. Itoh , C. R. Buell and T. Matsumoto. 2013. Improvement of the *Oryza sativa* Nipponbare reference genome using next generation sequence and optical map data. **Rice.** 6: 4.

Keller, B., C. Feuillet and N. Yahiaoui. 2005. Map-based isolation of disease resistance genes from bread wheat: cloning in a supersize genome. **Genet. Res**. 85: 93–100.

Kelsay, J. L., E. S. Prather, W. M. Clark and J. J. Canary. 1988. Mineral balances of man fed a diet containing fiber in fruits and vegetables and oxalic acid in spinach for six weeks. **J. Nutr.** 118: 1197-1204.

Klein, B., G. Weirich and H. Brauch. 2001. DHPLC-based germline mutation screening in the analysis of the VHL tumor suppressor gene: usefulness and limitations. **Hum Genet.** 108: 376–384.

KOME Report Search. 2004. **Ferritin, Knowledge-based Oryza Molecular biological Encyclopedia.** Available Source: http://cdna01.dna.affrc.go.jp/cgi-bin/cDNA/namazu.cgi?query=ferritin, March 21, 2004.

Komatsuda, T., M. Pourkheirandish, C. He, P. Azhaguvel, H. Kanamori, D. Perovic, N. Stein, A. Graner, T. Wicker, A. Tagiri, U. Lundqvist, T. Fujimura, M. Matsuoka, T. Matsumoto and M. Yano. 2007. Six-rowed barley originated from a mutation in a homeodomain-leucine zipper I-class homeobox gene. **Proc Natl Acad Sci**. 104: 1424–1429.

Koornneef, M., L. W. M. Dellaert and J. H. Van der veen. 1982. EMS- and radiation-induced mutation frequencies at individual loci in *Arabidopsis thaliana* L. **Heynh. Mutat. Res.** 93: 109-123.

Koike, S., H. Inoue, D. Mizuno, M. Takahashi, H. Nakanishi, S. Mori, N. K. Nishizawa. 2004. OsYSL2 is a rice metal-nicotianamine transporter that is regulated by iron and expressed in the phloem. **Plant J.** 39: 415–424.

Krattinger, S. G., T. Wicker, B. Keller. 2009. Map-based cloning of genes in Triticeae (wheat and barley) pp 337–357. *In* Muehlbauer G, Feuillet C (eds) Genetics and genomics of the triticeae, plant genetics and genomics. **Crops and models**. Springer Science+Business Media, LLC, pp 337–357.

Kumar, R., J. Qiu, T. Joshi, B. Valliyodan, D. Xu, and H. T. Nguyen. 2007. Single feature polymorphism discovery in rice. **PLoS ONE.** 2: e284.

Kurowska, M., A. Daszkowska-Golec, D. Gruszka, M. Marzec, M. Szurman, I.Szarejko and M. Maluszynski. 2011. TILLING - a shortcut in functional genomics. **J Appl Genetics**. 52: 371–390.

Laulhere, J.P. and J-F. Briat. 1993. Iron release and uptake by plant ferritin: effects of pH, reduction and chelation. **Biochem J.** 15(290): 693-699.

Lee, C. and D. L. Sedlak. 2009. A novel homogeneous Fenton-like system with Fe(III)–phosphotungstate foroxidation of organic compounds at neutral pH values. **J. Mol. Cat.** A: Chemical. 311: 1–6.

Lee, S., S. Lee, U.S. Jeon, S. J. Lee, Y.-K. Kim, D. P. Persson, S. Husted, J. K. Schjørring, Y. Kakei, Hi. Masuda, N. K. Nishizawa and G. Ana. 2009. Iron fortification of rice seeds through activation of the nicotianamine synthase gene. **Proc. Natl. Acad. Sci.** 106: 22014–22019.

Lobreaux, S., T. Hardy and J-F. Briat. 1993. Abscisic acid is involved in the iron-induced synthesis of maize ferritin. **The EMBO J**. 12: 651-657.

Lucca, P., R. Hurrell and I. Potrykus. 2001. Genetic engineering approaches to improve the bioavailability and the level of iron in rice grains. **Theor. Appl. Genet.** 102: 392 –397.

Prom-u-thai, C., D. Bernie, G. Thomson and R. Benjavan. 2003. Easy and rapid detection of iron in rice grain. **ScienceAsia.** 29: 203–207.

Marschner, H. and V. Römheld. 1994. Strategies of plants for acquisition of iron. **Plant Soil.** 165: 261–274.

Maser, P., S. Thomine, J. I. Schroeder, J. M. Ward, K. Hirschi, H. Sze, I. N. Talke, A. Amtmann, F. J. Maathuis, D. Sanders, J. F. Harper, J. Tchieu, M. Gribskov, M. W. Persans, D. E. Salt, S. A. Kim and M. L. Guerinot. 2001. Phylogenetic relationships within cation transporter families of *Arabidopsis*. **Plant Physiol**. 126: 1646-1667.

Masuda, H., K. Usuda, T. Kobayashi, Y. Ishimaru, Y. Kakei, M. Takahashi, K. Higuchi, H. Nakanishi, S. Mori, N.K. Nishizawa. 2009. Overexpression of the barley nicotianamine synthase gene *HvNAS1* increase iron and zinc concentrations in rice grains. **Rice.** 2: 155–166.

McCallum, C. M., L. Comai, E. A. Greene and S. Henikoff. 2000. Targeted screening for induced mutations. **Nat. Biotechnol.** 18(4): 55-57.

Marchler-Bauer, A., S. Lu, J. B. Anderson, F. Chitsaz, M. K. Derbyshire, C. DeWeese-Scott, J. H. Fong, L. Y. Geer, R. C. Geer, N. R. Gonzales, M. Gwadz, D. I . Hurwitz, J. D. Jackson, Z. Ke, C. J. Lanczycki, F. Lu, G. H. Marchler, M. Mullokandov, M. V. Omelchenko, C. L. Robertson, J. S. Song, N. Thanki, R. A. Yamashita, D. Zhang, N. Zhang, C. Zheng, S. H. Bryant. 2011. "CDD: a Conserved Domain Database for the functional annotation of proteins." **Nucleic Acids Res.** 39(D): 225-229.

Mori, S. 1999. Iron acquisition by plants. **Curr. Opin. Plant Biol.** 2: 250-253.

Nozoye T, S. Nagasaka, T. Kobayashi, M. Takahashi, Y. Sato, N. Uozumi, H. Nakanishi and N. K. Nishizawa. 2011. Phytosiderophore efflux transporters are crucial for iron acquisition in graminaceous plants. **J Biol Chem.** 286(7): 5446-5454.

Nishizawa, N. K., K. Bashir and Y. Ishimaru. 2010. Iron uptake and loading into rice grains. **Rice.** 3: 122–130.

Oefner, P. J. and P. A. Underhill. 1998. DNA mutation detection using denaturing high-performance liquid chromatography (DHPLC). **Current Protocols in Human Genetics.** Wiley & Sons, New York, Supplement 19:7.10.1-7.10.12.

Østergaard, L. and M. F. Yanofsky. 2004. Establishing gene function by mutagenesis in Arabidopsis thaliana. **Plant J**. 39: 682–696.

Rice, F. A. 1996. **Normal Iron Physiology: Iron absorption.** Iron Deficiency Anemia. Available Source: http://www.cariboo.bc.ca/schs/medtech/rice/irondeficiency.html, May 12, 2003.

Robinson, N. J., C. M. Procter, E. L. Connolly and M. L. Guerinot. 1999. A ferric-chelate reductase for iron uptake from soils. **Nature.** 397: 694-697.

Ruanjaichon, V., et al. 2013. Identification of genes confers high Fe and Fe toxic tolerance in rice. *In* **JST/BIOTEC report.** (Budget year 2012). National Center for Genetic Engineering and Biotechnology.

Rudolph, A., R. Becker, G. Scholz, Z. Procházka, J. Toman, T. Macek and V. Herout. 1985. The occurrence of the amino acid nicotianamine in plants and microorganisms. A reinvestigation. **Biochem. Physiol. Pflanzen.** 180: 557–563.

Schmidke, I. and U.W. Stephan. 1995. Transport of metal micronutrients in the phloem of castor bean (Ricinus communis) seedlings. **Physiol. Plant.** 95: 147–153.

Shojima, S., N. K. Nishizawa and S. Mori. 1989. Establishment of a cell-free system for the biosynthesis of nicotianamine. **Plant Cell Physiol.** 30: 673–677.

Sirichakwal, P., P. Puwastien, U. Yamborisut, M. Tontawiroon, R. Kongkachuichai, A. Kamchansuppasin, O. Pornaimmongkol. 2008. Efficacy Study of Iron-dense Rice Consumption on Iron Status in School Children With Iron Depletion *In* NRCT report. **Integrated Biotechnology in Developing Rice Strains for High Value-added and Nutritional Enrichment (**Budget year 2006). Kasetsart and Mahidol University.

Small, B. M. 2004. **Iron.** School of Medicine & Biomedicine Science. Available Source: http://www.smbs.buffalo.edu/med/hem/iron.pdf, September 7, 2004.

Small, I. 2007. RNAi for revealing and engineering plant gene functions. **Curr Opin Biotechnol.** 18: 148–153

Smith, J. L. 2004. **Current Topics: What roles do ferritin-like protein plays in bacteria?** Eastern Regional Research Center (ERRC), ARS, USDA. Available Source: http://www.arserrc.gov/mfs/current_topic.htm, July 20, 2004.

Takagi, S. 1976. Naturally occurring iron chelating compounds in oat- and rice-root washing. I. Activity measurement and preliminary characterization. **Soil Sci. and Plant Nutri.** 22: 423–433.

Takahashi, M., Y. Terada, I. Nakai, H. Nakanishi, E. Yoshimura, S. Mori, N. K. Nishizawa. 2003. Role of nicotianamine in the intracellular delivery of metals and plant reproductive development. **Plant Cell.** 15: 1263–1280.

Tadano, T. 1976. **Studies on the methods to prevent iron toxicity in the lowland rice.** Faculty of Agriculture Hokkaido University. 10 (1) 22-68.

Theil, E.C. 1987. Ferritin: structure, gene regulation, and cellular function in animals, plants, and microorganisms**. Annu. Rev. Biochem.** 56: 289- 315.

Thongbai, P. and B. A. Goodman. 2000. Free radical generation and post-anoxic injury in rice grown in an iron-toxic soil, pp. 1887–1900. **Ninth International Symposium on Iron Nutrition and Interactions in Plants**, Stuttgart, Germany.

Thongjuea, S., V. Ruanjaichon, R. Bruskiewich and A. Vanavichit. 2009. RiceGeneThresher: a webbased application for mining genes underlying QTL in rice genome. **Nucl Acids Res.** 37: D996–D1000.

Till, B. J., S. H. Reynolds, E. A. Greene, C. A. Codomo, L. C. Enns, J. E. Johnson, C. Burtner, A. R. Odden, K. Young, N. E. Taylor, J. G. Henikoff, L. Comai and S. Henikoff. 2003. Large-scale discovery of induced pointmutations with high-throughput TILLING. **Genome Res.** 13: 524–530

Tissue, B. M. 2013. Basics of analytical chemistry and chemical equilibria. John Wiley & Sons, Australia.

Trapnell, C., B. A. Williams, G. Pertea, A. Mortazavi, G. Kwan, M. J. van Baren, S. L. Salzberg, B. J. Wold and L. Pachter. 2010. Transcript assembly and abundance estimation from RNA-Seq reveals thousands of new transcripts and switching among isoforms. **Nat. Biotechnol.** 28(5): 511–515.

Tresca, A. J. 2004. **Facts About Iron:** What affects iron absorption? Irritable Bowel/ Crohn's Disease. Available Source: http://ibscrohns.about.com/cs/nutrition/a/fdairon.htm, June 17, 2004.

Tuntawiroon, M., N. Sritongkul, M. Brune, L. Rossander-Hulten, R. Pleehachinda, R. Suwanik and L. Hallberg. 1991. Dose dependent inhibitory effect of phenolic compounds in foodson non-heme iron absorption in men. **Am. J. Clin. Nutr.** 53: 554-57.

Upadhyaya, N. M., Q-H. Zhu and R. S. Bhat. 2011. Transposon insertional mutagenesis in rice, pp 147–177. *In* **Pereira A (ed) Plant reverse genetics, methods and protocols, methods in molecular biology.** Springer Science+Business Media, LLC.

Vanavichit, A., S. Tragoonrung, T. Toojinda, N. Phoka, A. Plabpla, S. Ruengphayak, S.Thongjua, N. Satakowit, E. Chaichumpoo and S. Phromphan. 2008. Improvement of High Nutrition Rice. *In* NRCT report. **Integrated Biotechnology in Developing Rice Strains for High Value-added and Nutritional Enrichment** (Budget year 2006). Kasetsart and Mahidol University.

Vance, D. B. 2002. Iron – the environment impact of the universal element. **Environmental Tech.** Available Source: http://2the4.net/iron.htm, February 18, 2004.

Vasconcelos, M., K. Datta, N. Oliva., M. Khalekuzzaman, L. Torrizo, S. Krishnan, M. Olivera, F. Goto and S. K. Datta. 2003. Enhanced iron and zinc accumulation in transgenic rice with the ferritin gene. **Plant Sci.** 164: 371-378.

Vazzola, V., A. Losa, C. Soave and I. Murgia. 2007. Knockout of frataxin gene causes embryo lethality in Arabidopsis. **FEBS Letters.** 581(4): 667-72.

Vert, G., J-F. Briat and C. Curie. 2001. *Arabidopsis IRT*2 gene encodes a root-periphery iron transporter. **Plant J.** 26: 181–189.

Ververk, K. 1959. Neutronic mutations in tomatoes. **Euphytica.** 8: 216-222.

Von Wirén, N., S. Klair, S. Bansal, J-F. Briat, H. Khodr, T. Shioiri, R. A. Leigh and R. C. Hider. 1999. Nicotianamine chelates both Fe III and Fe II. Implications for metal transport in plants. **Plant Physiol**. 119: 1107–1114.

Welch, R.M. 1995. Micronutrient nutrition of plants. **Crit. Rev. Plant Sci.** 14: 49–82.

Welz, B. and M. Sperling. 1999. **Atomic Absorption Spectrometry**. Wiley-VCH, Weinheim, Germany.

Werner, J. D., J. O. Borevitz, N. H. Uhlenhaut, J. R. Ecker, J. Chory, D. Weigel. 2005. FRIGIDA-independent variation in flowering time of natural *Arabidopsis thaliana* accessions. **Genetics**. 170: 1197–1207.

Wolyn, D. J., J. O. Borevitz, O. Loudet, C. Schwartz, J. Maloof, J. R. Ecker, C. C. Berry and J. Chory. 2004. Light-response quantitative trait loci identified with composite interval and extreme array mapping in *Arabidopsis thaliana*. **Genetics.** 167: 907–917.

Wu, J. L., C. Wu, C. Lei, M. Baraoidan, A. Bordeos, M. R. S. Madamba, M. R. Pamplona, R. Mauleon, A. Portugal, V. J. Ulat, R. Bruskiewich, G.Wang, J. Leach, G. Khush and H. Leung. 2005. Chemical- and irradiation-induced mutants of indica rice IR64 for forward and reverse genetics. **Plant Mol. Bio.** 59: 85–97.

World Health Organization (WHO). 2002. **World health report reducing risks, promoting healthy life.** Geneva.

Yang, R.Y. and S. C. S. Tsou. 2006. Enhancing iron bioavailability of vegetables through proper preparation−principles and applications. **J. International Cooperation.** 1(1): 107-119.

Yoshida S, D.A. Forno, J.H. Cock, K.A. Gomez. 1976. **Laboratory manual for physiological studies of rice**, 3rd edn. The International Rice Research Institute, Manila, Philippines.

Yu, S. and A. F. Yeager. 1960. Ten heritable mutations found in the tomato following irradiation with x-rays and thermal neutrons. **Proc. Am. Soc. Hortic. Sci.** 76: 538-542.

Zaharieva, T. and V. Römheld. 2001. Specific Fe^{2+} uptake system in Strategy I plants inducible under Fe deficiency. **Plant Nutr.** 23: 1733–1744.

Zhang, J. Y., Y. Lu, Y. Yuan, X. Zhang, J. Geng, Y. Chen, S. Cloutier, P.B.E. McVetty and G. Li. 2009. Map-based cloning and characterization of a gene controlling hairiness and seed coat color traits in *Brassica rapa*. **Plant Mol Biol.** 69: 553–563.

APPENDIX

Appendix Table 1 Iron bioavailability and nutritional profiles of 32 brown rice samples

Name	Harvesting date	Seed color	β-carotene µg/ 100 g	Lutein µg/ 100 g	Fe mg/ 100g	Zn mg/ 100g	Fe Bio ng ferritin	Phytate mg/ 100g	Poly-phenol mg/ 100g	Tanin mg tanic acid eqi/100g
Hom Nual (KDC4)	May 2008	white	11.69	5.16	1.34	3.38	10.38 ± 0.25	946.95	85.1	16.61
Klum Hom (KDC30)	May 2008	black	26.42	89.38	1.45	3.61	6.26 ± 0.26	1045.84	401.7	161.2
KDC 31-9-11-1-0	May 2008	white	8.29	11.74	1.75	4.4	3.56 ± 0.29	1236.29	57.3	17.63
(KDC 10) 23-2-7-2-3-0	Nov.2008	white	3.24	65.93	1.33	2.98	11.14 ± 0.46	999.53	74	24.1
(KDC 12) 23-2-14-1-1-0	Nov.2008	white	3.41	64.46	1.5	2.5	10.06 ± 0.47	1048.39	82.5	16.19
(KDC 19)23-2-14-5-3-0	Nov.2008	white	3.54	116.56	1.3	3.21	8.88 ± 0.23	953.97	90.8	29.31
(KDC 29)23-10-12-5-2-0	Nov.2008	white	3.45	52.28	1.3	3.42	3.24 ± 0.12	1149.68	82.9	23.66
(KDC 3) 18-3-17-1-19-0	Nov.2008	white	17.86	19.7	1.54	3.24	9.60 ± 0.46	1090.49	53.9	88.41
(KDC 33) 23-11-15-6-1-0	Nov.2008	white	-	-	1.3	3.7	10.32 ± 0.26	1128.43	75	26.68
(KDC 37) 23-12-1-4-3-0	Nov.2008	white	3.64	61.71	1.41	4.03	5.10 ± 0.10	1192.2	75.2	23.05
(KDC 5) 18-3-17-2-5-0	Nov.2008	white	2.56	55.23	1.92	3.24	9.26 ± 0.62	1004.84	54.3	27.21
(KDC 6) 18-3-17-3-3-0	Nov.2008	white	3.44	63.42	1.85	3.03	10.82 ± 0.75	975.77	51.6	26.56
(KDC43) 49-6-6-10-1-0	Nov.2008	black	-	-	1.62	4.27	2.12 ± 0.37	1169.71	134	161.36

Appendix Table 1 (Continued)

Name	Harvesting date	Seed color	β-carotene µg/ 100 g	Lutein µg/ 100 g	Fe mg/ 100g	Zn mg/ 100g	Fe Bio ng ferritin	Phytate mg/ 100g	Poly-phenol mg/ 100g	Tanin mg tanic acid eqi/100g
Pinkaset	May 2008	white	ND	ND	0.91	2.68	10.62 ± 0.37	1067.09	57.6	21.68
Pinkaset # 2	Dec. 2008	white	4.57	4.49	0.8	2.84	4.41 ± 0.36	1027.85	60.7	23.79
Pinkaset # 3	Dec. 2008	white	7.38	16.38	0.81	2.9	10.56 ± 1.46	989.88	62.2	20.51
IR71501/Pinkaset 3-1-14-20-0	Dec. 2008	white	2.68	4.94	1.01	2.6	7.46 ± 0.38	981.82	69.1	20.47
RD 6	ND	white	ND	ND	0.96	2.59	6.22 ± 0.42	1023.83	60.1	22.48
KDML105	Nov.2008	white	0.77	10.27	1.15	3.66	4.20 ± 0.22	1091.53	57.5	30.56
Sinlek	Oct. 2008	white	ND	9.67	1.32	3.62	5.40 ± 0.37	901.72	65.3	31.34
Sinlek KPS	May 2008	white	7.52	13.33	1.07	4.53	7.86 ± 0.73	1131.62	65.4	20.66
Sinlek Chiang Mai	May 2008	white	5.94	18.16	1.55	3.66	7.96 ± 0.27	1017.35	64.4	22.85
Riceberry	Dec. 2008	black	5.83	90.84	1.37	2.98	4.86 ± 0.34	911.86	316.3	139.15
Riceberry#2	May 2008	black	63.65	134.4	1.12	3.64	7.96 ± 0.62	1041.79	198.4	60.28
Riceberry	Aug. 2008	black	2.76	90.25	1.24	3.39	6.60 ± 0.45	907.43	194.7	73.36
KD/JHN 909-21-2-5	May 2008	white	3.9	5.07	1.01	3.24	5.48 ± 0.86	953.01	67.5	21.25

Appendix Table 1 (Continued)

Name	Harvesting date	Seed color	β-carotene µg/ 100 g	Lutein µg/ 100 g	Fe mg/ 100g	Zn mg/ 100g	Fe Bio ng ferritin	Phytate mg/ 100g	Poly-phenol mg/ 100g	Tanin mg tanic acid eqi/100g
JHN	Oct. 2008	black	1.44	66.29	1.31	3.86	4.28 ± 0.46	1018.77	123.4	53.4
Mu 4643	Oct. 2008	black	0.99	52.69	1.26	3.6	3.44 ± 0.15	1045.6	104.5	49.19
Mu 783	May 2008	black	-	-	1.41	2.94	10.52 ± 0.52	996.34	156.7	141.4
Mu FRO	May 2008	black	4.04	62.04	1.62	3.44	9.90 ± 0.45	1073.26	99.4	38.02
Basmati	Oct. 2008	white	1.57	12.23	1.22	3.97	4.80 ± 0.45	1109.73	43.1	51.29
IR68144	May 2008	white	16.69	36.72	1.53	3.92	2.96 ± 0.25	1158.63	69.6	22.89

Appendix Table 2 Sequence variation in two ferritin genes (*OsFer1* and *OsFer2*) among 7 rice varieties

Gene	Location on gene structure	Rice varieties						
		JHN	XBN	IR68144	BT#3	KD	Azu	Nip
OsFer1	upstream	A	A	A	A	G	G	G
OsFer1	upstream	T	T	T	T	C	C	C
OsFer1	upstream	G	G	G	G	A	A	A
OsFer1	upstream	G	G	G	G	A	A	A
OsFer1	upstream	G	G	G	G	A	A	A
OsFer1	upstream	ATATA TAGAT	ATATA TAGAT	ATATA TAGAT	ATATA TAGAT	-	-	-
OsFer1	upstream	C	C	C	C	T	T	T
OsFer1	upstream	G	G	G	G	A	A	A
OsFer1	upstream	G	G	G	G	A	A	A
OsFer1	upstream	A	A	A	A	G	G	G
OsFer1	upstream	T	T	T	T	G	G	G
OsFer1	upstream	G	G	G	G	C	C	C
OsFer1	upstream	C	C	C	C	A	A	A
OsFer1	Ex.2 (Synonymous)	G	G	G	G	A	A	A
OsFer1	downstream	G	G	G	G	C	C	C
OsFer1	downstream	T	T	T	T	-	-	-
OsFer1	downstream	A	A	A	A	G	G	G
OsFer1	downstream	G	G	G	G	A	A	A
OsFer1	downstream	A	A	A	A	C	C	C
OsFer2	upstream	G	nd	C	nd	G	nd	C
OsFer2	upstream	C	G	G	C	C	G	G
OsFer2	Ex.1 (Synonymous)	C	nd	G	nd	C	nd	G
OsFer2	downstream	A	A	G	A	A	G	G
OsFer2	downstream	C	N	T	N	C	T	T
OsFer2	downstream	C	C	G	C	C	G	G
OsFer2	downstream	A	A	G	A	A	G	G

Appendix Table 3 SFP polymorphic probes on low Fe density mutant (Mu8097)

Feature	Chr.	Loc.	Start-stop	Gene annotation	Gene ontology
Os.51661.1.S1_at	1	LOC_Os01g64330	37,348,349-37,351,043	retrotransposon protein, putative	retrotransposon protein
Os.12498.1.S1_at	1	LOC_Os01g72370	41,970,401-41,977,365	helix-loop-helix DNA-binding domain	transcription factor
Os.8888.1.S1_at	1	LOC_Os01g72934	42,300,756-42,301,320	hypothetical protein	hypothetical protein
Os.54396.1.S1_at	2	LOC_Os02g33944	20,221,158-20,229,251	transposon protein, CACTA, En/Spm sub-class	transposon protein
OsAffx.13539.1.S1_at	3	LOC_Os03g58260	33,186,605-33,190,969	Putative indole-3-glycerol phosphate lyase	Enzyme
Os.12218.1.S1_at	3	LOC_Os03g59050	33,605,332-33,610,651	DEAD-box ATP-dependent RNA helicase	Enzyme
OsAffx.25764.4.S1_at	3	LOC_Os03g59152	33,678,675-33,680,607	lethal leaf spot 1, putative	membrane protein
Os.17876.1.S1_at	3	LOC_Os03g59450	33,830,812-33,834,624	transporter-related, putative	membrane protein
Os.54163.1.S1_at	3	LOC_Os03g59460	33,835,705-33,838,079	transcription factor, putative	transcription factor
OsAffx.31328.1.S1_at	11	LOC_Os11g36679	21,187,888-21,191,567	zinc knuckle domain containing protein	uncharacterized protein
OsAffx.31370.1.S1_at	11	LOC_Os11g38490	22,347,609-22,349,764	hypothetical protein	hypothetical protein
OsAffx.7298.1.S1_at	11	LOC_Os11g35210	20,177,305-20,181,551	NB-ARC domain containing protein	signal transduction
OsAffx.19170.1.S1_at	11	LOC_Os11g35210	20,177,305-20,181,551	NB-ARC domain containing protein	signal transduction
OsAffx.7299.1.S1_at	11	LOC_Os11g35260	20,201,483-20,202,160	OsWAK118 - OsWAK receptor-like cytoplasmic kinase	transcription factor
Os.50237.1.S1_at	11	LOC_Os11g35840	20,565,230-20,570,633	Hypothetical protein	hypothetical protein
OsAffx.31316.1.S1_at	11	LOC_Os11g35850	20,574,742-20,577,936	expressed protein	Expressed protein
Os.10476.1.S1_at	11	LOC_Os11g35870	20,584,801-20,590,081	ExRWD domain containing protein	expressed protein
Os.54389.1.S1_at	11	LOC_Os11g36190	20,818,733-20,823,434	receptor kinase, putative	Enzyme
OsAffx.31324.1.S1_at	11	LOC_Os11g36410	21,002,628-21,006,037	NBS-LRR type disease resistance protein	ribosomal proteins
Os.8445.1.S1_at	11	LOC_Os11g36430	21,014,047-21,019,014	zinc finger, C_3HC_4 type domain containing protein	transcription factor
Os.50923.1.S1_at	11	LOC_Os11g36470	21,034,426-21,048,202	ubiquitin carboxyl-terminal hydrolase 21	Enzyme
Os.50853.1.S1_at	11	LOC_Os11g36480	21,058,689-21,061,052	zinc knuckle domain containing protein	transcription factor

Appendix Table 3 (Continued)

Feature	Chr.	Loc.	Start-stop	Gene annotation	Gene ontology
Os.52038.1.S1_at	11	LOC_Os11g36520	21,083,118-21,084,176	hypothetical protein	hypothetical protein
OsAffx.31338.1.S1_at	11	LOC_Os11g36560	21,100,507-21,106,142	zinc finger C3HC4 type family protein	transcription factor
OsAffx.31327.1.S1_at	11	LOC_Os11g36610	21,142,040-21,143,548	OsFBDUF51 - F-box and DUF domain	transcription factor
OsAffx.7317.1.S1_s_at	11	LOC_Os11g36810	21,262,123-21,263,086	hypothetical protein	hypothetical protein
Os.53491.1.S1_at	11	LOC_Os11g36830	21,264,689-21,266,932	expressed protein	expressed protein
OsAffx.7318.1.S1_at	11	LOC_Os11g36930	21,317,535-21,322,904	ZOS11-05 - C2H2 zi nc finger protein	transcription factor
OsAffx.31338.3.S1_at	11	LOC_Os11g36960	21,339,976-21,343,407	dnaJ domain containing protein	membrane protein
Os.51985.2.A1_at	11	LOC_Os11g37050	21,405,934-21,410,956	expressed protein	expressed protein
Os.51985.1.S1_at	11	LOC_Os11g37050	21,405,934-21,410,956	expressed protein	expressed protein
Os.51985.1.S2_at	11	LOC_Os11g37050	21,405,934-21,410,956	expressed protein	expressed protein
OsAffx.7320.1.S1_at	11	LOC_Os11g37160	21,469,799-21,470,917	hypothetical protein	hypothetical protein
OsAffx.7328.3.S1_at	11	LOC_Os11g37610	21,733,281-21,736,517	hypothetical protein	hypothetical protein
Os.5349.1.S1_at	11	LOC_Os11g37700	21,806,691-21,816,309	PDR-like ABC transporter	membrane protein
Os.18929.1.S1_s_at	11	LOC_Os11g38580	22,396,318-22,401,139	NBS-LRR type disease resistance protein	signal transduction
Os.39008.1.S1_at	11	LOC_Os11g38610	22,410,270-22,418,418	Expressed protein	expressed protein
Os.49419.1.S1_at	11	LOC_Os11g39160	22,839,736-22,847,294	NBS-LRR disease resistance protein	signal transduction
Os.52807.1.S1_at	11	LOC_Os11g39209	22,880,524-22,882,449	expressed protein	expressed protein
OsAffx.31383.1.S1_at	11	LOC_Os11g39300	22,932,731-22,935,416	hypothetical protein	hypothetical protein
Os.50270.1.S1_at	11	LOC_Os11g39310	22,937,286-22,941,152	NB-ARC domain, putative	signal transduction
Os.49419.2.S1_at	11	LOC_Os11g39320	22,941,973-22,946,899	LZ-NBS-LRR class, putative, expressed	signal transduction
Os.49419.1.S1_at	11	LOC_Os11g39320	22,941,973-22,946,899	LZ-NBS-LRR class, putative	signal transduction
OsAffx.7353.1.S1_at	11	LOC_Os11g39350	22,955,587-22,960,560	expressed protein	expressed protein
Os.20727.1.S1_at	11	LOC_Os11g39650	23,148,907-23,153,185	WD domain, G-beta repeat domain	signal transduction

Appendix Table 4 SFP polymorphic probes on high Fe density mutant (Mu4643)

Feature	Chr.	Loc.	Start-stop	Gene annotation	Gene ontology
Os.18166.1.S1_at	3	LOC_Os03g18540	10,380,274-10,386,518	Expressed protein	Expressed protein
Os.21893.3.A1_at	8	LOC_Os08g31980	19,827,615-19,833,374	trehalose-6-phosphate synthase	Enzyme
Os.23006.1.S1_at	2	LOC_Os02g58200	35,615,875-35,616,373	Expressed protein	Expressed protein
Os.27457.1.S1_at	4	LOC_Os04g02890	1,124,261-1,130,522	Expressed protein	Expressed protein
Os.31879.1.S1_at	3,7,9,10	-	-	Expressed protein	Expressed protein
Os.36453.1.S1_at	1	-	30269806-30270682	-	-
Os.38751.1.A1_at	3,4,5,10,11,12	-	-	B1075D06.13	-
Os.45173.1.S1_x_at	1,2,4,7,8,11,12	-	-	hypothetical protein	hypothetical protein
Os.46208.1.S1_s_at	10,C	LOC_Os10g38276	20,411,008-20,411,751	chloroplast ATP synthase	Enzyme
Os.49465.1.S1_at	10	LOC_Os10g17520	8,765,959-8,767,010	Expressed protein	Expressed protein
Os.50394.1.S1_at	9	LOC_Os09g09350	5,004,955-5,005,589	Expressed protein	Expressed protein
Os.51633.1.S1_x_at	9	LOC_Os09g04924	2,639,763-2,642,481	Expressed protein	Expressed protein
Os.52531.1.S1_at	5	LOC_Os05g23230	13,201,109-13,202,884	Expressed protein	Expressed protein
Os.52861.1.S1_at	2,7,10	-	-	New cDNA-based Gene	-
Os.53213.1.S1_x_at	11	LOC_Os11g34130	19,519,583-19,523,024	Expressed protein	Expressed protein
Os.54723.1.S1_at	9	LOC_Os03g25140	14,358,019-14,369,428	peptidyl-prolyl isomerase	Enzyme
Os.8490.1.S1_at	1,3	-	-	Os01g0923400 protein	uncharacterized protein
OsAffx.10645.2.S1_x_at	1	LOC_Os01g67070	38,937,859-38,938,416	hypothetical protein	hypothetical protein
OsAffx.17400.1.S1_at	1,4,6	-	-	Hypothetical protein	Hypothetical protein
OsAffx.20673.1.A1_at	5,6,10	-	-	retrotransposon protein	retrotransposon protein

Appendix Table 4 (Continued)

Feature	Chr.	Loc.	Start-stop	Gene annotation	Gene ontology
OsAffx.21416.1.S1_at	1	-		hypothetical protein	hypothetical protein
OsAffx.29148.1.S1_at	8	LOC_Os08g11240	6,606,946-6,607,826	hypothetical protein	hypothetical protein
OsAffx.31018.3.S1_x_at	1,2,4,5	-	-	Expressed protein	Expressed protein
OsAffx.32192.1.S1_x_at	2,4,10,C	-	-	Photosystem II M protein	signal transduction
OsAffx.32195.1.A1_at	4,7,8,9,10,C	-	-	Ribosomal protein	signal transduction
OsAffx.32259.1.A1_at	1,2,6,10,12,C	-	-	Chloroplast ORF230	signal transduction
OsAffx.32325.1.A1_at	4,10,12,C	-	-	Maturase	Enzyme
OsAffx.32347.1.S1_x_at	2,4,6,C	-	-	Photosystem II protein	signal transduction
OsAffx.6484.1.A1_at	9	LOC_Os09g35590	20,456,609-20,457,019	hypothetical protein	hypothetical protein
OsAffx.8236.1.S1_x_at	1,2,4,10,C	-	-	ORF100	uncharacterized protein
OsAffx.8734.1.S1_at	7	-	3630487-3631291	hypothetical protein	hypothetical protein
OsAffx.8882.1.S1_at	1,2,5	-	-	Hypothetical protein	hypothetical protein

Appendix Table 5 Genotyping of the 28 bp insertion on *OsLLS1* and 10 bp insertion on *OsFer1* among 23 standard cultivars and iron mutants

Name	28 bp insertion on *OsLLS1*	10 bp insertion on *OsFer1*
Pinkaset#2	cgccgtcgtggctgcggctgtgctgtgc	atatatagat
Pinkaset#3	nd	nd
Pinkaset+4_1E06	nd	atatatagat
Pinkaset+4_66B09	nd	nd
KDML105	nd	nd
Suphanburi1	nd	nd
PSM	nd	atatatagat
Nippornbare	nd	nd
BLB resistant#497	nd	nd
KD-Rathu	nd	nd
KD_BLB	nd	nd
Sinlek	nd	nd
Riceberry	nd	atatatagat
JHN	nd	atatatagat
Riceberry#2	nd	nd
Homcholasit	nd	atatatagat
Homnual	nd	nd
IR68144	cgccgtcgtggctgcggctgtgctgtgc	atatatagat
IR64	nd	nd
IR1188	nd	nd
Nivara#91	nd	nd
Basmati	nd	atatatagat/-
KDC6_11_2	nd	nd
Mu4643	nd	atatatagat
Mu4906	nd	atatatagat
MuFRO	nd	atatatagat
Mu9396	nd	atatatagat
Mu1255	nd	atatatagat
Mu10599	nd	atatatagat
Mu8097	cgccgtcgtggctgcggctgtgctgtgc	atatatagat
JHN	nd	atatatagat
Mu2491	cgccgtcgtggctgcggctgtgctgtgc	atatatagat
Mu2538	cgccgtcgtggctgcggctgtgctgtgc	atatatagat
Mu3130	nd	atatatagat
MuMT1	nd	atatatagat
Mu11183	cgccgtcgtggctgcggctgtgctgtgc	atatatagat

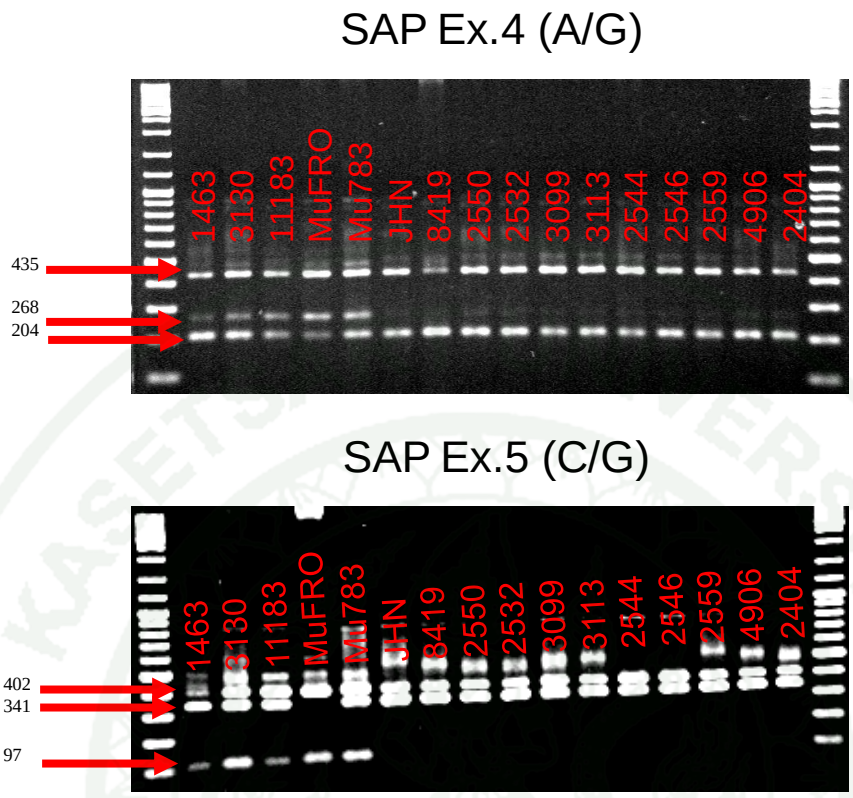

Appendix Figure 1 Genotyping iron toxic mutants using the Bi-directional SNP primers for a Single Amino Acid Change (SAP) on exon 4 and 5

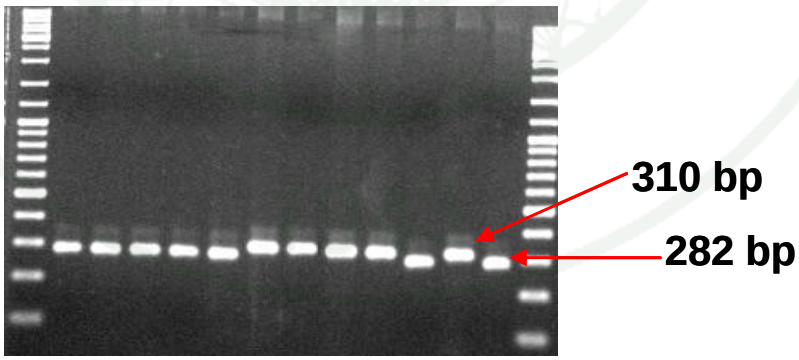

Appendix Figure 2 Genotyping of The 28 bp insertion located on *OsLLS1*. Expected amplicon sizes of indel were 282 or 310 bp

CIRRICULUM VITAE

NAME : Mr. Siriphat Ruengphayak

BIRTH DATE : April 08, 1981

BIRTH PLACE : Samut Songkhram

EDUCATION :

YEAR	INSTITUTE	DEGREE/DIPLOMA
2002	Kasetsart Univ., Thailand	B.S. (Agriculture)

POSITION/TITLE : Assistant Researcher

WORK PLACE : Rice Science Center

SCHOLARSHIP/ AWARDS: The Royal Golden Jubilee (RGJ)-PhD program Grant No. PHD / 0009 / 2546, from the Thailand Research Fund (TRF)